Decadal change of summertime reactive oxidized nitrogen and surface ozone over the Southeast United States

Jingyi Li[1], Jingqiu Mao[2], Arlene M. Fiore[3], Ronald C. Cohen[4,5], John D. Crounse[6], Alex P. Teng[6], Paul O. Wennberg[6,7], Ben H. Lee[8], Felipe D. Lopez-Hilfiker[8], Joel A. Thornton[8], Jeff Peischl[9,10], Ilana B. Pollack[11], Thomas B. Ryerson[9], Patrick Veres[9,10], James M. Roberts[9], J. Andrew Neuman[9,10], John B. Nowak[12,a], Glenn M. Wolfe[13,14], Thomas F. Hanisco[14], Alan Fried[15], Hanwant B. Singh[16], Jack Dibb[17], Fabien Paulot[18,19], Larry W. Horowitz[19]

[1]Jiangsu Key Laboratory of Atmospheric Environment Monitoring and Pollution Control, Collaborative Innovation Center of Atmospheric Environment and Equipment Technology, School of Environmental Science and Engineering, Nanjing University of Information Science and Technology, Nanjing, Jiangsu, 210044, China

[2]Department of Chemistry and Biochemistry & Geophysical Institute, University of Alaska Fairbanks, Fairbanks, Alaska, 99775, USA

[3]Department of Earth and Environmental Sciences & Lamont-Doherty Earth Observatory of Columbia University, Palisades, New York, 10027, USA

[4]Department of Chemistry, University of California, Berkeley, Berkeley, California, 94720, USA

[5]Department of Earth and Planetary Science, University of California, Berkeley, Berkeley, California, 94720, USA

[6]Division of Geological and Planetary Sciences, California Institute of Technology, Pasadena, California, 91125, USA

[7]Division of Engineering and Applied Science, California Institute of Technology, Pasadena, California, 91125, USA

[8]Department of Atmospheric Sciences, University of Washington, Seattle, Washington, 98195, USA

[9]Chemical Sciences Division, NOAA Earth System Research Laboratory, Boulder, Colorado, 80305, USA

[10]Cooperative Institute for Research in Environmental Science, University of Colorado Boulder, Boulder, Colorado, 80309, USA

[11]Department of Atmospheric Science, Colorado State University, Fort Collins, Colorado, 80523, USA

[12]Aerodyne Research, Inc., Billerica, Massachusetts, 01821, USA

[13]Joint Center for Earth System Technology, University of Maryland Baltimore County, Baltimore, Maryland, 21250, USA

[14]Atmospheric Chemistry and Dynamics Lab, NASA Goddard Space Flight Center, Greenbelt, Maryland, 20771, USA

[15]Institute of Arctic & Alpine Research, University of Colorado, Boulder, Colorado, 80309, USA

[16]NASA Ames Research Center, Moffett Field, California, 94035, USA

[17]Department of Earth Sciences and Institute for the Study of Earth, Oceans, and Space, University of New Hampshire, Durham, New Hampshire, 03824, USA

[18]Program in Atmospheric and Oceanic Sciences, Princeton University, Princeton, New Jersey, 08544, USA

[19]Geophysical Fluid Dynamics Laboratory/National Oceanic and Atmospheric Administration, Princeton, New Jersey, 08540, USA

[a]now at: NASA Langley Research Center, Hampton, Virginia, USA

Correspondence to: Jingqiu Mao (jmao2@alaska.edu)

Abstract

Widespread efforts to abate ozone (O_3) smog have significantly reduced nitrogen oxides (NO_x) emissions over the past two decades in the Southeast U.S. (SEUS), a place heavily influenced by both anthropogenic and biogenic emissions. How reactive nitrogen speciation responds to the reduction in NO_x emissions in this region remains to be elucidated. Here we exploit aircraft measurements from ICARTT (July-August, 2004), SENEX (June-July, 2013), and SEAC^{4}RS (August-September, 2013) and long-term ground measurement networks alongside a global chemistry-climate model to examine decadal changes in summertime reactive oxidized nitrogen (RON) and ozone over the Southeast U.S. We show that our model can well reproduce the mean vertical profiles of major RON species and the total (NO_y) in both 2004 and 2013. Among the major RON species, nitric acid (HNO_3) is dominated (~ 42 – 45 %), followed by NO_x (31 %), total peroxy nitrates (∑PNs; 14 %), and total alkyl nitrates (∑ANs; 9 – 12 %) on a regional scale. We find that most RON, including NO_x, ∑PNs and HNO_3 decline proportionally with decreasing NO_x emissions in this region, leading to a similar decline in NO_y. This linear response might be in part due to the nearly constant summertime supply of biogenic VOC emissions in this region. Our model captures the observed relative change of RON and surface ozone from 2004 to 2013. Model sensitivity tests indicate that further reductions of NO_x emissions will lead to a continued decline in surface ozone and less frequent high ozone events.

1 Introduction

Since the 1990s, the U.S.A. Environmental Protection Agency (U.S. EPA) has targeted emissions of nitrogen oxides (NO_x) to improve air quality by lowering regional photochemical smog (The 1990 Clean Air Amendment). Satellite- and ground-based observations imply significant declines in U.S. NO_x emissions, with a decreasing rate of roughly - 4 % yr^{-1} after 2005 (Krotkov et al., 2016; Russell et al., 2012; Tong et al., 2015; Miyazaki et al., 2017; Lu et al., 2015; Lamsal et al., 2015). This has proven effective at lowering near-surface ozone (O_3) in the past few decades (Cooper et al., 2012; Simon et al., 2015; Hidy and Blanchard, 2015; Stoeckenius et al., 2015; Xing et al., 2015; Yahya et al., 2016; Astitha et al., 2017). The average of the annual 4th highest daily maximum 8-h average (MDA8) ozone over 206 sites has decreased by 31 % from 101 ppb in 1980 to 70 ppb in 2016 across the continental U.S., with more significant reductions in rural areas of the eastern U.S. in summer (Simon et al., 2015; Cooper et al., 2012). Here we use both aircraft and ground-based datasets, combined with a high resolution chemistry-climate model, to evaluate responses of reactive oxidized nitrogen (RON) and surface ozone to the NO_x emission reductions in the Southeast U.S.

In the troposphere, ozone is produced through photochemical reactions involving NO_x and volatile organic compounds (VOCs) in the presence of sunlight. During photooxidation, a large fraction of NO_x is transformed into its reservoirs, including nitric acid (HNO_3),

peroxy nitrates (RO_2NO_2; dominated by peroxyacetyl nitrate (PAN)), and alkyl nitrates ($RONO_2$). These species, together with NO_x, are known as total reactive oxidized nitrogen ($NO_y = NO_x + HNO_3 + HONO + 2 \times N_2O_5$ + total peroxy nitrates ($\sum$PNs) + total alkyl nitrates ($\sum$ANs)). Some of these reservoir species, particularly those with an organic component, tend to be less soluble and longer lived. They may carry reactive nitrogen far from the NO_x source region (Stohl et al., 2002; Parrish et al., 2004; Li et al., 2004) and thereby affect NO_x concentrations and O_3 formation on a regional to global scale (Liang et al., 1998; Horowitz et al., 1998; Perring et al., 2013; Paulot et al., 2016; Hudman et al., 2004).

$RONO_2$ originating from biogenic VOCs (BVOCs) represents a major uncertainty in the NO_y budget, as BVOC emissions account for more than 80 % of global VOC emissions (Millet et al., 2008). To a large extent, this is due to the uncertainties in current understanding of BVOC oxidation chemistry. Biogenic $RONO_2$ species are mainly produced from the oxidation of BVOCs by OH in the presence of NO_x during daytime and by nitrate radical (NO_3) during nighttime. Laboratory and field studies show a wide range of $RONO_2$ yields from their BVOC precursors (Browne et al., 2014; Fry et al., 2014; Lockwood et al., 2010; Paulot et al., 2009; Rindelaub et al., 2015; Rollins et al., 2009; Lee et al., 2014; Xiong et al., 2015; Xiong et al., 2016; Teng et al., 2015). Another uncertainty lies in the fate of $RONO_2$, i.e. recycling $RONO_2$ into NO_x or converting it to HNO_3 have important implications for the NO_y budget and thus O_3 production (Fiore et al., 2005; Horowitz et al., 2007; Ito et al., 2009; Perring et al., 2013; Paulot et al., 2012). This is further complicated by particle-phase $RONO_2$, an important component of secondary organic aerosol (SOA) over the Southeast U.S. (Xu et al., 2015; Lee et al., 2016). The fate of particle-phase $RONO_2$ is unclear, with the possibility for removal by hydrolysis to form HNO_3 (Jacobs et al., 2014; Hu et al., 2011; Darer et al., 2011; Rindelaub et al., 2015; Szmigielski et al., 2010; Sato, 2008; Romer et al., 2016; Wolfe et al., 2015; Boyd et al., 2017; Boyd et al., 2015; Bean and Hildebrandt Ruiz, 2016), photochemical aging (Nah et al., 2016), and deposition (Nguyen et al., 2015). To what extent $RONO_2$ affect the partitioning of RON and surface ozone remains to be elucidated.

Extensive datasets in the Southeast U.S. offer a great opportunity to study the decadal change of RON and surface ozone, resulting from NO_x emission decline. Aircraft campaigns during the summers of 2004 and 2013, including the International Consortium for Atmospheric Research on Transport and Transformation (ICARTT) (Fehsenfeld et al., 2006; Singh et al., 2006), the Southeast Nexus (SENEX) (Warneke et al., 2016), and the Studies of Emissions and Atmospheric Composition, Clouds and Climate Coupling by Regional Surveys (SEAC^{4}RS) (Toon et al., 2016), provide detailed characterization of tropospheric composition in this region separated by nearly a decade. These data have been widely used to evaluate model estimates of RON and ozone (Singh et al., 2007; Pierce et al., 2007; Perring et al., 2009; Fischer et al., 2014; Hudman et al., 2007; Henderson et al.,

2011; Hudman et al., 2009; Edwards et al., 2017; Baker and Woody, 2017; Travis et al., 2016; Mao et al., 2013b; Fisher et al., 2016; Yu et al., 2016; Liu et al., 2016). Together with measurements from networks, including the National Atmospheric Deposition Program (NADP) and EPA Air Quality System (AQS), these datasets enable a close examination of responses of RON and surface ozone to NO_x emissions reduction in this region.

Here we use a high-resolution global 3D climate-chemistry model, the Geophysical Fluid Dynamics Laboratory (GFDL) AM3 model, with updated isoprene and organic nitrate chemistry to investigate decadal changes of RON and surface O_3 during summer between 2004 and 2013 over the Southeast U.S. We first evaluate the model with comprehensive measurements from three aircraft campaigns in the summer of 2004 (ICARTT) and 2013 (SENEX and SEAC^{4}RS). Model estimates of nitrate wet deposition flux are also evaluated against measurements from NADP; model estimates of NO_y are compared with measurements from EPA AQS to provide an additional constraint on the fate of RON in the model. We then investigate the repartitioning of RON in response to NO_x emission reductions from 2004 to 2013 on a regional scale. From there, we examine the model estimate of decadal changes of summertime surface O_3 at 157 EPA AQS monitoring sites over the Southeast U.S. We also demonstrate the sensitivity of RON and MDA8 O_3 to a hypothetical NO_x emission reduction over the next decade.

2 Methodology

2.1 AM3 Model

We apply a high-resolution (50 x 50 km^2) version of the GFDL AM3 global chemistry-climate model to study decadal changes of RON and O_3 over the Southeast U.S. Chemistry-climate models provide a unique capability to both evaluate model representation of these observed changes and use that to improve future projections of air quality in the same region. The model configuration is to a large extent similar to that used in another paper (Li et al., 2016); and a short summary is provided below. The dynamical core, physical parameterizations, cloud and precipitation processes, and cloud-aerosol interactions mainly follow Donner et al. (2011), except that convective plumes are computed on a vertical grid with finer resolution (Paulot et al., 2016). Dry deposition in the model has been updated to use dry deposition velocities calculated in the GEOS-Chem model (Paulot et al., 2016), to reflect rapid deposition of organic nitrates and oxidized volatile organic compounds (OVOCs) (Nguyen et al., 2015). The current time step for chemistry and transport in our model is 20 mins. We show below in section 4.1 that, with the current setting, our model can well reproduce the vertical profiles of RON. Sensitivity of RON to operator duration should refer to Philip et al. (2016).

Isoprene emissions are computed in the model using the Model of Emissions of Gases and Aerosols from Nature (MEGAN). In 2004, isoprene emissions over the continental U.S. (25-50° N, 130-70° W) are computed to be 8.0 Tg C in July and August together, with a previous model estimate of 7.5 Tg C by Mao et al. (2013b). In 2013, model estimates of isoprene emissions were scaled down by 20% following Li et al. (2016). The resulting isoprene emissions are 7.7 Tg C in July-August in this region, with little difference compared to 2004. Monoterpene emissions follow Naik et al. (2013) and do not vary interannually, with a total of 4.0 Tg C in July and August.

Anthropogenic emissions follow the Representative Concentration Pathway 8.5 (RCP 8.5) projection (Lamarque et al., 2011) for both 2004 and 2013, to compare the model to observations in a consistent fashion and also enable future projection of air quality in this region. As shown in Table 1, anthropogenic NO_x emissions over the continental U.S. during July-August of 2004 amount to 0.42 Tg N mon^{-1}, consistent with Hudman et al. (2007) but 11 % lower than EPA estimates of 0.47 Tg N mon^{-1} (Granier et al., 2011). For the year of 2013, we apply a 25 % reduction to the anthropogenic NO_x emissions from the RCP 8.5 projection (from base year of 2010), to best reproduce the vertical profiles of RON during SENEX as shown below in section 4.1. This adjustment is also consistent with recent estimates of NO_x emissions over the Southeast U.S. (Anderson et al., 2014). The resulting anthropogenic NO_x emissions (0.25 Tg N mon^{-1}) are 14 % lower than NEI11v1 emission inventory estimate of 0.29 Tg N mon^{-1} (0.28 Tg N mon^{-1} from the updated NEI11v2 emission inventory), although both inventories have a similar spatial distribution (Figure S1). We also apply a diurnal variation to anthropogenic NO_x emissions following Mao et al. (2013b). Soil NO_x emissions in our model, 3.6 Tg N yr^{-1} globally (Naik et al., 2013), are considerably lower than other model estimates, including 5.5 Tg N yr^{-1} in Yienger and Levy (1995) and 9.0 Tg N yr^{-1} in Hudman et al. (2012). As a result, the anthropogenic NO_x emissions over the continental U.S. are 0.84 Tg N for July-August of 2004, and 0.50 Tg N in July-August of 2013, with 40 % reduction from 2004 to 2013 (Table 1). This relative change in anthropogenic NO_x emissions is consistent with EPA estimates (https://www.epa.gov/air-emissions-inventories/air-pollutant-emissions-trends-data) and satellite observations (Krotkov et al., 2016; Lu et al., 2015). Compared to the NEI11v1 inventory, RCP 8.5 used in our model shows similar relative differences in both national and Southeast region.

2.2 Gas-phase chemistry

We apply the same isoprene mechanism as described by Li et al. (2016). A full list of the reactions can be found in Table S1. This mechanism is based on Mao et al. (2013b), but has been significantly revised to incorporate recent laboratory updates on isoprene oxidation by OH, O_3 and NO_3 (Schwantes et al., 2015; Bates et al., 2016; Peeters et al., 2014; St. Clair et al., 2016; Bates et al., 2014; Praske et al., 2015; Müller et al., 2014; Lee et al., 2014; Crounse et al., 2011). One major feature is the suppression of δ-isoprene

hydroxyl peroxy radical (δ-$ISOPO_2$) and subsequent reaction pathways in the model, as these channels are considered to be of minor importance under ambient conditions (Peeters et al., 2014; Bates et al., 2014). The fraction of $ISOPO_2$ undergoing isomerization is calculated using bulk isomerization estimates (Crounse et al., 2011). As a result, the first-generation isoprene alkyl nitrate is assumed to be β-hydroxy nitrate (ISOPNB) in the model with a yield of 10 % from the $ISOPO_2$ + NO pathway. This differs from a recent GEOS-Chem study of organic nitrates over the Southeast U.S. that assumed 9 % yield of the first-generation isoprene alkyl nitrate comprised of 90 % ISOPNB and 10 % δ-hydroxy nitrate (ISOPND) (Fisher et al., 2016). The treatment of β- and δ-$ISOPO_2$ will not only affect the speciation of organic nitrates but also the production of O_3 due to different NO_x recycling efficiency in their secondary products. We also include updated chemistry for methylvinyl ketone (MVK) (Praske et al., 2015), an updated yield of hydroxy hydroperoxides (ISOPOOH) (Bates et al., 2016; St. Clair et al., 2016), fast photolysis of carbonyl organic nitrates (Müller et al., 2014), and an updated ozonolysis rate of ISOPNB (Lee et al., 2014). In addition, we reduce the yield of organic nitrates (MACRN) from methacrolein (MACR) oxidation from 15 % to 3 %, which is estimated from the measured yield of nitrate from MVK oxidation (Praske et al., 2015).

Another major model revision involves the treatment of nighttime oxidation of isoprene. Instead of following Mao et al. (2013b), we revised nighttime oxidation of isoprene largely based on the Leeds Master Chemical Mechanism v3.2 (MCM v3.2), allowing a more complete description of isoprene oxidation by NO_3. In particular, MCM v3.2 suggests significant production of propanone nitrate (PROPNN) from the photooxidation of the C_5 carbonyl nitrate, consistent with recent laboratory experiments (Schwantes et al., 2015). We also updated the products of the reaction of nitrooxy alkylperoxy radical (INO_2), the peroxy radical from isoprene oxidation by NO_3, with HO_2 to reflect a lower molar yield (0.77) of C_5 nitrooxy hydroperoxide (INPN) (Schwantes et al., 2015). The differences between MCM v3.2 and the most updated version, MCM v3.3.1, in isoprene nighttime chemistry appears to be small (Jenkin et al., 2015). We therefore use MCM v3.2 as the reference in this work.

We include a highly simplified chemistry for the oxidation of monoterpenes in this work, mainly to quantify their contribution to organic nitrates. Monoterpenes are lumped into one chemical species ($C_{10}H_{16}$) in our model. The organic nitrate yield is set to 26 % from OH-initiated oxidation (Rindelaub et al., 2015) and to 10 % from NO_3-initiated oxidation (Browne et al., 2014). Details of the monoterpene chemistry can be found in Table S2.

2.3 Heterogeneous loss of organic nitrates

Field and laboratory studies have indicated a potential contribution to aerosol formation of organic nitrates from BVOC oxidation (Ayres et al., 2015; Fry et al., 2014; Nah et al., 2016; Rollins et al., 2009; Rindelaub et al., 2015; Boyd et al., 2015; Lee et al., 2016; Ng et al.,

2008; Fry et al., 2009; Xu et al., 2015; Lee et al., 2014; Bean and Hildebrandt Ruiz, 2016; Spittler et al., 2006; Boyd et al., 2017). Aerosol yield depends on both the VOC precursor and the oxidant. For example, Δ-3-carene oxidation by NO_3 can produce a 38-65 % yield of organic aerosols in a smog chamber (Fry et al., 2014), which is much higher than the 1-24 % yield from NO_3-initiated isoprene oxidation (Ng et al., 2008; Rollins et al., 2009; Ayres et al., 2015). Recent chamber studies indicate a very low aerosol yield from α-pinene oxidation by NO_3 (Nah et al., 2016; Fry et al., 2014), the aerosol yield increases to ~ 18 % when α-pinene is oxidized by OH (Rollins et al., 2010; Rindelaub et al., 2015). However, these results might not be representative of atmospheric conditions in terms of the RO_2 reaction partner or RO_2 lifetime, warranting further studies on the effects of RO_2 fates on aerosol formation (Boyd et al., 2017; Boyd et al., 2015; Ng et al., 2008; Schwantes et al., 2015).

In the condensed phase, organic nitrates can undergo hydrolysis reactions producing HNO_3 (Darer et al., 2011; Hu et al., 2011; Rindelaub et al., 2015; Boyd et al., 2015; Szmigielski et al., 2010; Sato, 2008; Jacobs et al., 2014; Bean and Hildebrandt Ruiz, 2016). However, the hydrolysis rate varies greatly with the structure of nitrate (Bean and Hildebrandt Ruiz, 2016; Darer et al., 2011; Hu et al., 2011; Boyd et al., 2015; Rindelaub et al., 2016). Here we assume a first-order irreversible reactive uptake for the heterogeneous loss of organic nitrates onto aerosols (R1), followed by its hydrolysis reaction returning HNO_3 and alcohols (R2) (Fisher et al., 2016):

$$RONO_2(g) \xrightarrow{k_1} AONJ(aq) \quad \text{(R1)}$$

$$AONJ(aq) + H_2O \xrightarrow{k_2} ROH + HNO_3(g) \quad \text{(R2)}$$

where $RONO_2$, AONJ and ROH represent gas- and particle-phase organic nitrates and alcohols respectively. We allow heterogeneous loss of organic nitrates to sulfate, black carbon, primary organic carbon, sea salt, mineral dust and SOA following Mao et al. (2013a). Besides the base case that only includes ISOPNB for heterogeneous loss (Jacobs et al., 2014), we include two additional sensitivity tests to evaluate the potential impact of organic nitrate hydrolysis. One is "hydro_full" case including heterogeneous loss of a C_5 dihydroxy dinitrate (DHDN) and monoterpene nitrates only from OH oxidation during daytime (TERPN1; nighttime monoterpene nitrates are excluded), and the other one is "no_hydro" case assuming no heterogeneous loss for any organic nitrates. We adopt an effective uptake coefficient 0.005 for ISOPNB and DHDN, and 0.01 for TERPN1, following Fisher et al. (2016), with a 3-h bulk lifetime in particle phase (Pye et al., 2015; Lee et al., 2016) (Table S3). Details of each case are listed in Table 2.

3 Observational datasets

We use measurements from a series of field campaigns (2004 ICARTT, 2013 SENEX, and 2013 SEAC^{4}RS) to evaluate model performance on O_3, NO_x, HNO_3, PAN, $\sum$ANs and NO_y over the Southeast U.S. in summer.

The ICARTT aircraft campaign provided a detailed characterization of tropospheric chemistry over the eastern U.S. in the summer of 2004 (July 1 - August 15, 2004). Two aircrafts, the NASA DC-8 and the NOAA WP-3D, were deployed to collect measurements of ozone, RON, isoprene and its oxidation products. Here we focus on data including O_3, NO_x, HCHO (Tunable Diode Laser (TDL) absorption spectrometry), HNO_3 (mist chamber/IC by University of New Hampshire and Chemical Ionization Mass Spectrometer (CIMS) by California Institute of Technology), PAN and $\sum$ANs (including gas and aerosol $RONO_2$) collected on the NASA DC-8 aircraft over the Southeast U.S. Details of the instrument operation and accuracy are summarized in Singh et al. (2006) and references therein.

Two aircraft campaigns were conducted in the summer of 2013 over the Southeast U.S. The first one is NOAA SENEX campaign, using NOAA WP-3D aircraft to investigate the interaction between biogenic and anthropogenic emissions and the formation of secondary pollutants (May 27 - July 10, 2013). We focus on daytime measurements of O_3, NO_x, HNO_3, PAN, speciated $RONO_2$ and NO_y in this work. Details of the instrument operation and accuracy are summarized in Warneke et al. (2016) and references therein. The second one is NASA SEAC^{4}RS campaign, which took place in August - September of 2013, with a focus on vertical transport of atmospheric pollutants from the surface to the stratosphere. Here we focus on observations of O_3, NO_2, HCHO (laser-induced fluorescence, LIF), $\sum$ANs (including gas and aerosol $RONO_2$) and speciated $RONO_2$ collected on NASA DC-8 aircraft to evaluate model representation of $\sum$ANs and several $RONO_2$ originating from isoprene oxidation. Details of the instrument operation and accuracy are summarized in Toon et al. (2016) and references therein.

Besides these aircraft campaigns, we also use surface observations for model evaluation, including nitrate (NO_3^-) wet deposition flux and concentration from the National Trends Network (NTN) of NADP (accessible at http://nadp.sws.uiuc.edu/data/) and surface O_3 and NO_y from EPA AQS (accessible at https://aqs.epa.gov/aqsweb/documents/data_mart_welcome.html). We focus on NO_3^- wet deposition fluxes at 53 NADP sites and MDA8 O_3 at 157 EPA AQS sites (Figure S2) in the Southeast U.S. during July - August of 2004 and 2013. NO_y measurements at 10 out of the 157 AQS sites in the same episodes are compared with model estimates as an additional constraint on the decadal change of NO_y. We choose July – August as our 'summer' since this is the common period of all the measurements used in model evaluation.

4 Model evaluation

We evaluate our model against observations from aircraft campaigns in 2004 and 2013. For each of the three field campaigns, all measurements are averaged to a 1-min time resolution. Data from biomass burning ($CH_3CN \geq 225$ ppt or $HCN \geq 500$ ppt), urban plumes ($NO_2 \geq 4$ ppb or $NO_x/NO_y \geq 0.4$ (if NO_y is available)), and stratospheric air ($O_3/CO > 1.25$ mol mol^{-1}) are excluded (Hudman et al., 2007) in all the analyses, as these subgrid processes may not be well represented in our model. We focus on the Southeast U.S. region, using data within the domain of 25 - 40° N latitude and 100 - 75° W longitude for our analyses. A map of all the flight tracks of each campaign is shown in Figure S3. All model results are sampled along the flight track with 1-min time resolution.

4.1 Mean vertical profiles of O_3 and RON

Figure 1 shows the observed and modeled mean vertical profiles of O_3, NO_x, HNO_3, PAN, ∑ANs and NO_y during ICARTT and SENEX. We use ∑ANs measurements from SEAC^{4}RS to evaluate model performance during summer 2013, due to the lack of ∑ANs measurements from SENEX. Our model results include both gas and aerosol $RONO_2$ in ∑ANs, although aerosol $RONO_2$ accounts for 7~11% of ∑ANs in the planetary boundary layer (PBL, < 1.5 km). We do not consider inorganic nitrates in particle phase in this analysis, due to lack of thermodynamic model for inorganic aerosols in current version of AM3. This simplification is expected to have minimal effects, as they only account for a small fraction of aerosol nitrates in the Southeast U.S. (Ng et al., 2017). To investigate the impact of $RONO_2$ hydrolysis, we include two model simulations, the base case with heterogeneous loss of ISOPNB, and a sensitivity run 'no_hydro' without heterogeneous loss of organic nitrates.

Mean observed O_3 in the surface layer decreased from 50 ppb during ICARTT to 35 ppb during SENEX, consistent with the declining trend in surface MDA8 ozone at AQS monitoring sites (section 5.2). As we show in section 5.2, this decline in ozone is mainly driven by NO_x emission reduction, with little influence by meteorology in the two years. Our model can reproduce the vertical gradient and the relative change of O_3 from 2004 to 2013, except for a positive absolute bias of 6 - 12 ppb in the boundary layer. Performance statistics of O_3 in the boundary layer listed in Table S4 also indicate positive biases in the model, with the fractional bias (FB) of 9.4 – 17%, fractional error (FE) of 16 – 19 %, normalized mean bias (NMB) of 9.4 – 16% and normalized mean error (NME) of 16 – 19 %. This overestimate of O_3 is higher than that reported (3 - 5 ppb) by Mao et al. (2013b) for their simulation of the ICARTT dataset, likely due to faster photolysis of carbonyl nitrates that increases the NO_x recycling efficiency from isoprene oxidation.

We further examine mean vertical profiles of NO_x and its reservoirs in 2004 and 2013 (Figure 1). In the boundary layer along the flight tracks, HNO_3 is the most abundant RON, accounting for 40 - 46 % of NO_y, followed by NO_x (18 - 23 %), PAN (20 %), and ∑ANs

(11 - 21 %). Between 2004 and 2013, mean observed NO_y in the boundary layer decreased by 20 %, from 2.0 ppb to 1.6 ppb, a weaker change than the 35 % reduction of total NO_x emissions (Table 1). The responses of major RON are mostly proportional to the change in NO_x emissions, with the notable exception of ∑ANs. We find significant decreases in NO_x (- 35 %) and HNO_3 (- 29 %) as well as a slight decrease in PAN (- 13 %) from observations. The relative trends of HNO_3 and PAN are opposite to those found in the Los Angeles (LA) basin, where PAN decreased much faster than HNO_3 (Pollack et al., 2013). This difference results mainly from the rapid decrease of anthropogenic VOC emissions in the LA basin that also serves as major precursors of PAN. In contrast, isoprene is the major precursor of PAN over the Southeast U.S. Its emissions show a constant supply (within 5 % differences over the two summers) in this region. ∑ANs shows a different trend from the above compounds, increasing from 0.23 ppb to 0.27 ppb (+ 17 %) near the surface. As we show below in section 5.1, these changes (except for ∑ANs) are mostly consistent with model estimates on a regional average. Discrepancy in their trends of vertical profiles and regional average might be due to representative errors from the three aircraft campaigns on spatial (Figure S3) and temporal (different episodes, referring to observation data description in section 3) scales.

The model can well reproduce RON in the boundary layer but tend to underestimate them in the free troposphere. This is likely due to insufficient production of NO_x from lightning in the free troposphere in our model, which is 0.048 Tg N in total over North America during July - August of 2004, lower by almost a factor of 5 compared to the value (0.27 Tg N from July 1-August 15, 2004) reported by Hudman et al. (2007). This underestimate can be improved by scaling up lightning emission by a factor of 5-10 (Fang et al., 2010). We do not adjust the lightning NO_x emissions in this work due to its high uncertainty (Ott et al., 2010; Pickering et al., 1998).

Hydrolysis of organic nitrates affects $RONO_2$ significantly in the boundary layer. By introducing hydrolysis of ISOPNB, we find that model relative bias of ∑ANs is reduced from + 20 % to + 2 % during ICARTT (Figure 1). Performance metrics in Table S4 also indicate better agreement of the model with observations if hydrolysis of ISOPNB assumed. However, the relative bias is increased in magnitude from – 9 % to – 24 % during SEAC^{4}RS. This low bias can be partially due to neglecting small alkyl nitrates, which could contribute 20 - 30 ppt to ∑ANs (less than 10% near the surface) during SEAC^{4}RS (Fisher et al., 2016). Including small alkyl nitrates will increase modeled ∑ANs a bit in ICARTT as well. Hydrolysis of ISOPNB also leads to a slight increase of HNO_3 (Table S4). The impact of hydrolysis of ISOPNB on boundary layer O_3 appears to be small. This is mainly because without hydrolysis, the dominant loss of ISOPNB is oxidation by OH, which then leads to the formation of secondary organic nitrates including MVKN, MACRN and DHDN. The majority of these organic nitrates (MVKN and DHDN) return NO_x slowly due to their long lifetimes (Table S5), resulting in a similar effect on ozone production as hydrolysis of

ISOPNB. In addition to the good agreement of ∑ANs, our model shows good agreement with speciated $RONO_2$ measured during SENEX and SEAC^{4}RS, including ISOPN and the sum of MVKN and MACRN (Figure 2). We find that the large discrepancy between ∑ANs and speciated alkyl nitrates (Figure S4) can be explained by a combination of monoterpene nitrates and DHDN and nighttime NO_3 oxidation products from isoprene, accounting for 20 - 24 %, 14 - 17 % and 23 - 29 % of ∑ANs respectively in the boundary layer.

Given the good agreement between observed and modeled RON in both 2004 and 2013, we find that the ozone bias, shown in Figure 1, cannot be completely explained by an overestimate of anthropogenic NO_x emissions. A recent GEOS-Chem study (Travis et al., 2016) shows that the ozone bias in their model can be largely reduced by scaling down anthropogenic NO_x emissions. We find that a similar reduction of anthropogenic NO_x emissions in 2013, from 0.25 Tg N mon^{-1} to 0.15 Tg N mon^{-1}, would lead to an underestimate of NO_y, HNO_3 and PAN by 30 %, 33 % and 30 %, respectively. Such a reduction would be also inconsistent with the relative changes in EPA estimates of NO_x emissions shown above. Indeed, other processes, such as ozone dry deposition, may also contribute to this bias and warrant further investigation.

4.2 NO_3^- wet deposition flux and concentration

Figure 3 shows a comparison of NO_3^- wet deposition flux between observations and model results during the summers of 2004 and 2013. The observed NO_3^- wet deposition flux is calculated by multiplying the measured NO_3^- concentration and precipitation at each monitoring site as $F_{o,i}=C_{o,i}P_{o,i}$, where $F_{o,i}$ is the monthly-mean NO_3^- wet deposition flux, $C_{o,i}$ and $P_{o,i}$ are the monthly-mean observed NO_3^- concentration precipitation at monitoring site i. The modeled NO_3^- wet deposition flux includes HNO_3 and all the alkyl nitrates. Observations indicate a 24 % reduction of NO_3^- wet deposition flux in summer from 2004 to 2013 over the Southeast U.S., likely due to NO_x emission reductions. This reduction in monthly averaged NO_3^- wet deposition flux is well captured by our model (-29 %), despite a low relative bias of 40 % in both years and NMB of - 39 – - 43 % (Table S4).

Since errors in modeled precipitation could strongly affect the modeled NO_3^- wet deposition flux (Appel et al., 2011; Grimm and Lynch, 2005; Metcalfe et al., 2005; Paulot et al., 2014; Tost et al., 2007), we also evaluate the modeled NO_3^- concentration ($C_{p,i}$), which is calculated by using the modeled NO_3^- wet deposition flux ($F_{p,i}$) and observed precipitation ($P_{o,i}$; $C_{p,i}=F_{p,i}/P_{o,i}$), as a separate constraint. The model shows a similar declining trend from the observations with a relative bias of - 23 % and – 41 % on NO_3^- concentration for 2004 and 2013 respectively. Our results are consistent with the base case of Paulot et al. (2016), which showed that convective removal is likely insufficient in AM3, leading to underestimates of both NO_3^- wet deposition flux and concentrations. Our results are somewhat different from a recent GEOS-Chem study (Travis et al., 2016). They found that

reducing anthropogenic NO_x emissions from NEI11v1 by 53 % can significantly improve the overestimate of 71 % on NO_3^- wet deposition flux in their model during August-September of 2013. A further reduction of anthropogenic NO_x emissions in our model (to 0.15 Tg N mon^{-1}), as suggested by Travis et al. (2016), would lead to an even greater negative bias compared to observations.

4.3 $RONO_2$ and related species

We further evaluate $RONO_2$ and related species in this section, with a large focus on measurements from ICARTT and SEAC^{4}RS. The major pathway for the production of daytime $RONO_2$ is the reaction of NO with RO_2 originating from VOC oxidation by OH:

$$RH + OH + O_2 \rightarrow RO_2 + H_2O \quad \text{(R3)}$$

$$NO + RO_2 \rightarrow (1 - \alpha)\, NO_2 + \alpha\, RONO_2 + HCHO + \text{products} \quad \text{(R4)}$$

where α is the branching ratio for alkyl nitrate formation. NO_2 subsequently undergoes photolysis to produce O_3:

$$NO_2 + h\nu \xrightarrow{O_2} O_3 + NO \quad \text{(R5)}$$

For isoprene, α is 9 ± 4 % (for ISOPN) according to a recent study (Xiong et al., 2015). For monoterpenes, specifically α-pinene, α ranges from 1 % to 26 % (Rindelaub et al., 2015; Nozière et al., 1999; Aschmann et al., 2002). Here, we use 10 % for isoprene and 26 % for monoterpenes. As $RONO_2$ and O_3 are both produced from (R4), a correlation between them is expected. We show that the model can roughly reproduce the correlation of O_x (= O_3 + NO_2) vs. ∑ANs during both ICARTT and SEAC^{4}RS (Figure 4), although the slope has a positive relative bias of about 21 % and 33 % respectively, largely due to an overestimate of O_3 in the model. The good agreement between observed and modeled O_x vs. daytime $RONO_2$ provides additional support for our treatment of the yields and fate of these daytime isoprene nitrates.

Another metric to evaluate $RONO_2$ chemistry is the correlation between ∑ANs and HCHO, as the latter is a coproduct from (R4). We show in Figure 4 that the model can roughly capture the observed ∑ANs-HCHO slope, with an underestimate by 25 % and 13 % during ICARTT and SEAC^{4}RS, respectively. The underestimate is in part due to small alkyl nitrates that are neglected in the model, as mentioned in section 4.1. During ICARTT, the slope estimated by AM3 is 0.12, similar to the value (0.15) from a previous GEOS-Chem study using a different isoprene oxidation mechanism that assumed a higher α (of 4.7% from ISOPNB and 7.0% from ISOPND vs. 10 % of ISOPNB and zero ISOPND in AM3) and a lower yield of HCHO (66 % vs. 90 % in AM3) (Mao et al., 2013b). The reason for such similarity between the two models might be two-fold: (a) the additional contribution

of monoterpene nitrates to ∑ANs in AM3 compensates for the decrease in α from isoprene nitrates compared to GEOS-Chem and (b) the coarse grid resolution of GEOS-Chem simulation (2° x 2.5°) may lead to a higher estimate of HCHO compared to the result from a finer grid resolution (Yu et al., 2016).

Since HCHO can be produced from other pathways of isoprene hydroxyl peroxy radicals ($ISOPO_2$) besides (R4) (such as isomerization of $ISOPO_2$ and $ISOPO_2 + HO_2$), changes in the slope of ∑ANs vs. HCHO may help to quantify decadal changes in isoprene oxidation pathways. We find in Figure 4 that the observed slope of ∑ANs-HCHO shows very little change from 2004 to 2013. This is in part due to substantial HCHO production from isoprene oxidation under low NO_x conditions (Li et al., 2016), and in part due to the buffering of ∑ANs in response to decreasing NO_x, as shown below in section 5.1. Our model is able to reproduce such behavior. We also find that the branching ratios for the reactions of $ISOPO_2$ change marginally from 2004 to 2013 over the Southeast U.S. (Figure S5). The fraction of $ISOPO_2 + NO$ has decreased from 81 % in 2004 to 66 % in 2013. The fraction of $ISOPO_2 + HO_2$ has increased from 15 % to 28 %, and the fraction of $ISOPO_2$ isomerization has increased from 4 % to 6 %. Our result is slightly different from the results of GEOS-Chem, which found a lower contribution from the NO pathway (54 %) and higher from isomerization (15 %) during August - September of 2013 (Travis et al., 2016).

We also compare the correlation between major daytime isoprene nitrates and HCHO during 2013, which provides a constraint on the yield of these nitrates. Our model shows a slight overestimate on the slope (Figure 4 (b)), consistent with comparison of mean vertical profiles shown in Figure 2. The computed slope (5 %) in this study is different from that (2.5 %) of a recent GEOS-Chem simulation by Fisher et al. (2016). This is partially due to the different treatment of β- and δ-$ISOPO_2$ between GEOS-Chem and AM3. Another factor is that MVKN and MACRN are not allowed to hydrolyze in AM3, leading to higher abundance of these two nitrates.

Figure 5 shows the mean vertical profiles of modeled monoterpene nitrates (MNs) and isoprene nitrates (INs) during ICARTT and SEAC^{4}RS. INs are the most abundant $RONO_2$, accounting for 76-80 % below 3 km over the Southeast U.S. In the measurements, ISOPN + MVKN + MACRN only contribute one third of the total INs (Figure S4). We show below that the discrepancy of ∑ANs and speciated $RONO_2$ can be explained by other daytime and nighttime INs as well as MNs in the model. More than 60 % of modeled INs originate from isoprene oxidation during daytime. The first-generation nitrate ISOPN contributes slightly more (31 %) than the second-generation nitrates MVKN + MACRN (28 %) to the total daytime INs during ICARTT. This is different from Mao et al. (2013b) who showed a higher contribution of MVKN + MACRN than the first-generation INs, due to the different treatment of β- and δ-$ISOPO_2$. We see more ISOPN (32 %) than MVKN + MACRN (26 %) from the daytime INs during SEAC^{4}RS, consistent with Fisher et al. (2016). A large

uncertainty in our model is attributed to DHDN, which contributes 32 % to the daytime INs. Fisher et al. (2016) showed less DHDN during SEAC^{4}RS since it was removed rapidly by hydrolysis (1-h lifetime) in their model. Our sensitivity test (hydro_full, Figure S6) indicates that AM3 would significantly underestimate ∑ANs if we assume a similar heterogeneous loss of DHDN as ISOPN. In fact, DHDN was hypothesized originally in Lee et al. (2014) for the imbalance of nitrogen in their lab experiments, and may serve as a proxy for a large number of unidentified daytime INs. It remains unclear what the dominant loss of DHDN is. Daytime nitrates from monoterpene oxidation are another important source of ∑ANs in this region, accounting for 17 - 20 % (24 - 26 ppt) of the total. Fisher et al. (2016) estimate a smaller burden of MNs, of about 10 - 20 ppt due to a lower molar yield (18 % vs. 26 % in AM3) and faster hydrolysis of MNs in their model.

Nighttime chemistry contributes about 30 - 36 % of ∑ANs, which is dominated by isoprene oxidation as well (Figure 5). 33 - 41 % of the INs are produced during night, similar to the value (44 %) reported by Mao et al. (2013b) but with different speciation, due to the different treatment of chemistry. PROPNN contributes about 29-38 % of the total INs. PROPNN in this work is mainly produced from the oxidation of C5 nitrooxy hydroperoxide (INPN) and C5 carbonyl nitrate (ISN1; dominantly by photolysis) that are generated from isoprene oxidation by NO_3 during the nighttime. This is different from Fisher et al. (2016), who showed that PROPNN is partially from the δ-$ISOPO_2$ + NO pathway and partially from the oxidation of ISN1 by NO_3. In our model, we see a rapid increase of PROPNN after sunrise in the boundary layer (Figure S7), consistent with observations at the Southern Oxidants and Aerosols Study (SOAS) ground site CTL (Schwantes et al., 2015). Our model overestimates the mean vertical profile of PROPNN by a factor of 3 (not shown). As our model may largely underrepresent the chemical complexity of nighttime isoprene oxidation as shown by Schwantes et al. (2015), we consider PROPNN as a proxy for other unspecified isoprene nighttime nitrates. Over all, PROPNN contributes a significant fraction of ∑ANs in the model, 23 - 29 % in the boundary layer as shown in section 4.1. With monoterpene nitrates and isoprene derived DHDN and nighttime NO_3 oxidation products taken into account, we find that model can well reproduce both observed ∑ANs and speciated alkyl nitrates (Figure S4).

5 Decadal Change of PBL RON and surface ozone over SEUS

As RON and related species from aircraft and surface measurements are well reproduced in our model for both 2004 and 2013, we assume that the model is representative of this chemical environment, and then use the model to derive monthly mean changes between 2004 and 2013. We also investigate the impacts of further decreases in NO_x emissions by applying a hypothetical 40 % reduction of anthropogenic NO_x emissions of 2013 but keeping other emissions and meteorology the same ("hypo" case in Table 2).

5.1 RON

We first examine the simulated decadal change of RON in the boundary layer over the Southeast U.S. as shown in Figure 6. In summer of 2004, the model suggests that NO_y is mainly comprised of HNO_3 (45 %), NO_x (31 %), ∑PNs (14 %) and ∑ANs (9 %). In response to a 40 % reduction in anthropogenic NO_x emissions (35 % reduction in total NO_x emissions, Table 1) from 2004 to 2013, NO_y declined by 34 %. This modeled response is comparable to long-term NO_y measurements from the AQS surface network, which shows on average a 45 % decrease from 2004 to 2013 over the Southeast U.S. Based on model estimates in Figure 6, most RON are reduced proportionally, with decreases of 38 % for HNO_3, 32 % for NO_x and 34% for ∑PNs. The different change in ∑PNs and PAN (the majority of ∑PNs) in Figure 1 might be due to the difference in sampling regions. The only exception is ∑ANs, with a smaller decline of 19 %. As an important source of organic aerosols (OA), ∑ANs may contribute to the decrease of OA over the Southeast U.S. in the past decade (Blanchard et al., 2016).

We conducted a sensitivity test with an additional 40 % reduction of anthropogenic NO_x emissions from 2013. We find that NO_y decreases by 29 %, with a proportional decrease in HNO_3, NO_x, and ∑PNs (Figure 6). The slower decrease of NO_y is likely due to ∑ANs, which decrease at a slower rate and becomes a larger fraction of NO_y. The buffering of ∑ANs is consistent with previous studies (Browne and Cohen, 2012; Fisher et al., 2016), mainly due to lower OH resulting from decreased NO_x (Figure S8) and thus a prolonged lifetimes of NO_x and ∑ANs (Browne and Cohen, 2012). As shown in Figure S8, averaged noontime OH decreases by 11 % from 2004 to 2013 and by 29 % after we impose an additional 40 % NO_x emission reduction from 2013 levels.

The historical NO_x emission reduction also affects reactive nitrogen export out of the boundary layer. Here we define exported nitrogen as the difference of the sources (chemical production and emissions) and sinks (chemical loss, wet and dry deposition). As shown in Table 3, total summertime NO_y export from the Southeast U.S. boundary layer decreases proportionally, from 24.1 Gg N in 2004 to 16.6 Gg N in 2013. The NO_y export efficiency, calculated as net exported nitrogen divided by total NO_x emissions, remains roughly the same (12 %) for 2004 and 2013, comparable to previous studies (Fang et al., 2010; Li et al., 2004; Parrish et al., 2004; Mao et al., 2013b; Sanderson et al., 2008; Hudman et al., 2007). Among all exported species, NO_x contributes most of net export from the PBL (6 % of total NO_x emissions), followed by PAN (4 %) and ∑ANs (2 %). We emphasize in Table 3 that a major fraction of NO_x is exported through the top of the boundary layer (convection). From a budget calculation throughout the tropospheric column over the same region, we find that despite being the same NO_y export efficiency (12 %), HNO_3 becomes the major exporter, accounting for half of NO_y export efficiency from the total column (6 %). The contributions from PAN and ∑ANs are roughly the same as their export from the boundary layer (4 % and 2 %). This suggests that surface NO_x ventilated through the boundary layer, converted to HNO_3 in the free troposphere and

exported as HNO_3 is likely the major NO_y export mechanism over the Southeast U.S. in our model, which is in agreement with previous observations (Parrish et al., 2004; Neuman et al., 2006). PAN and ∑ANs together account for another half of NO_y export efficiency. As PAN and ∑ANs are of biogenic origin and longer lived than HNO_3, they may play a key role in influencing RON and ozone in downwind regions (Moxim et al., 1996; Fischer et al., 2014).

5.2 Surface ozone

Since the mid-1990s, NO_x emission controls have led to significant improvement on ozone air quality over the eastern U.S. (Simon et al., 2015; Cooper et al., 2012). As NO_x emissions continue to decrease, ozone production efficiency (OPE) may increase due to the lower NO_x removal rate by OH and to some extent may compensate the ozone reduction (Sillman, 2000). Meanwhile, surface ozone production may be further complicated by the increasing importance of RO_2 isomerization and $RO_2 + HO_2$. Here we first evaluate our model against surface ozone observations in 2004 and 2013, and then project the future response of surface ozone to even lower NO_x emissions to examine the efficacy of near-term NO_x emission controls at lowering near-surface ozone levels.

We first examine the modeled surface ozone against observations at 157 EPA AQS monitoring sites over the Southeast U.S. in July-August of 2004 and 2013 (Figure S9). In general, AM3 overestimates surface MDA8 ozone in both years by about 16 ppb on average, with the NMB of 33 - 45 % and NME of 35 - 46 % respectively. This positive bias of summertime surface O_3 has been a common issue to a number of modeling studies of this region (Fiore et al., 2009; Canty et al., 2015; Brown-Steiner et al., 2015; Strode et al., 2015; Travis et al., 2016). This might be partially attributed to overestimated anthropogenic NO_x emissions from non-power plant sectors, excessive vertical mixing in the boundary layer (Travis et al., 2016) or underestimates of O_3 dry deposition (Hardacre et al., 2015; Val Martin et al., 2014). Further studies are warranted to investigate the cause of this bias in AM3.

Surface O_3 concentrations over the Southeast U.S. decline substantially from 2004 to 2013 in response to the large NO_x emission reduction (Simon et al., 2015). MDA8 ozone averaged across all the monitoring sites is observed to decrease by 11 ppb (23 % of observed mean MDA8 ozone in July-August of 2004) resulting from approximately 40 % reductions of anthropogenic NO_x emissions (35 % reduction in total NO_x emissions). This strong sensitivity of surface ozone to NO_x emission reflects the linear relationship between ozone production rate and NO_x concentrations when NO_x is low (Trainer et al., 2000). Our model is able to capture this strong NO_x - O_3 sensitivity, with the mean MDA8 ozone reduced by 10 ppb from 2004 to 2013. We find that a further 40 % reduction of anthropogenic NO_x emissions with identical meteorological conditions could lead to an additional 9 ppb decrease, a similar magnitude to the change from 2004 to 2013.

We further investigate the impact of temperature and moisture on surface O_3 from 2004 to 2013. While several studies suggest that surface O_3 increases with ambient temperature (Jacob and Winner, 2009; Bloomer et al., 2010; Wu et al., 2008; Steiner et al., 2010), Cooper et al. (2012) showed that this temperature related impact is weak during the period of 1990-2010 across the U.S.A. Recent studies suggest that relative humidity (RH) or vapor pressure deficit (VPD) may play an important role in ozone variability through soil-atmosphere or biosphere-atmosphere coupling (Kavassalis and Murphy, 2017; Camalier et al., 2007; Tawfik and Steiner, 2013). Our model shows marginal differences in RH (less than 1 %) and temperature (+ 2.4 K) within the PBL over the Southeast U.S. between the summers of 2004 and 2013, consistent with observed changes of RH (+ 2.7 %) and temperature (+ 2.6 K) during ICARTT and SENEX. This small variation in the model is also consistent with climatology data (Hidy et al., 2014). Camalier et al. (2007) showed that RH has a much bigger impact on summertime ozone than temperature over the Southeast U.S., suggesting little influence of meteorology on ozone trend. Using the same model but with the standard AM3 chemical mechanism, Lin et al. (2017) found that meteorology changes would have caused high surface ozone over the eastern U.S. to increase by 0.2 - 0.4 ppb yr^{-1} in the absence of emission controls from 1988 to 2014. Therefore, we conclude that the impact of climate variability and change on O_3 is relatively small compared to NO_x emission reductions over the Southeast U.S., consistent with previous studies (Lam et al., 2011; Hidy et al., 2014; Lin et al., 2017; Rieder et al., 2015).

Decreasing NO_x emissions also reduces the frequency of high O_3 pollution events. Figure 7 shows the probability density function of observed and modeled MDA8 ozone at each monitoring site during July-August of 2004 and 2013, and the probability density function of modeled MDA8 ozone under a hypothetical scenario with another 40 % reduction in anthropogenic NO_x emissions compared to 2013. We show that the lowest O_3, about 20 ppb in current model simulations, remains invariant with NO_x emission changes over the Southeast U.S., consistent with observations (Figure 7 (a)). Meanwhile, the high tail of MDA8 ozone events has shifted from more than 100 ppb in 2004 to about 85 ppb after the 40 % reduction of anthropogenic NO_x emissions from 2013. A similar shift is found in observations. The narrowing of the range of O_3 with decreasing NO_x is consistent with the observed trends reported by Simon et al. (2015). We also find that further reductions of NO_x emissions will reduce both median O_3 values and the high tail, suggesting that fewer high ozone events will occur under continued NO_x emission controls in the future.

6 Conclusions and Discussions

Near-surface ozone production over the Southeast U.S. is heavily influenced by both anthropogenic and biogenic emissions. We investigate the response of NO_y speciation to the significant NO_x emission controls (about 40 % reduction) in this region over the past decade, in light of the fast-evolving understanding of isoprene photooxidation. This knowledge is needed to predict nitrogen and ozone budgets in this region and elsewhere in

643 the world with similar photochemical environments. Here we use extensive aircraft and
644 ground observations, combined with a global chemistry-climate model (GFDL AM3), to
645 examine decadal changes in NO_y abundance and speciation as well as in surface O_3 mixing
646 ratios over the Southeast U.S. between the summers of 2004 and 2013. We then use the
647 model to infer future NO_y speciation and surface ozone abundances in response to further
648 NO_x emission controls in this region.

649 We first evaluate the model with aircraft and surface observations. When we apply the
650 estimated 40 % reductions in anthropogenic NO_x emissions from 2004 to 2013, our model
651 reproduces the major features of vertical profiles of NO_x, HNO_3, PAN, $\sum$ANs and NO_y
652 observed during aircraft campaigns over the Southeast U.S. in the summers of 2004 and
653 2013. By including recent updates to isoprene oxidation, our model can largely reproduce
654 the vertical profiles of $\sum$ANs and several speciated alkyl nitrates, as well as their
655 correlations with O_x and HCHO, lending support to the model representation of isoprene
656 oxidation. On the other hand, we show that a discrepancy between measured $\sum$ANs and
657 speciated $RONO_2$ can be explained by a combination of monoterpene nitrates, dinitrates
658 and nighttime NO_3 oxidation products from isoprene. We also show that modeled ozone
659 appears to be insensitive to hydrolysis of ISOPNB, because its photooxidation, mainly by
660 OH, also returns little NO_x.

661 Major RON decline proportionally as a result of NO_x emission reductions in the Southeast
662 U.S., except for a slower rate in $\sum$ANs. The slower decline of $\sum$ANs reflects the prolonged
663 lifetime of NO_x when it is decreasing. Our model suggests that summertime monthly
664 averaged NO_x, HNO_3, PAN, and NO_y decline by 30 - 40 %, in response to 40 % reduction
665 in anthropogenic NO_x emissions from 2004 to 2013. This proportional decrease is likely
666 driven by high concentrations of biogenic VOCs, the major precursor of PAN in this region
667 that change little in magnitude from 2004 to 2013. In contrast, Pollack et al. (2013) find a
668 faster PAN decrease than HNO_3 in the LA basin over the past several decades, partly due
669 to the decrease in anthropogenic VOC emissions that are major PAN precursors.

670 Deposited and exported NO_y decline with NO_x emission reductions. The model also shows
671 a decrease of NO_3^- wet deposition flux by 29 % from 2004 to 2013, consistent with
672 observations from the NADP network (- 24 %). We find from model calculations that the
673 NO_y export efficiency remains at 12 % in both 2004 and 2013, leading to a proportional
674 decrease of exported NO_y. The dominant NO_y export terms include NO_x or HNO_3, each
675 accounting for 6% of the total exported NO_y, followed by $\sum$PNs (4 %) and $\sum$ANs (2 %).

676 The response of surface ozone to NO_x emission reductions reveals a strong $NO_x - O_3$
677 sensitivity in summertime over the Southeast U.S. Observations from EPA AQS surface
678 network suggest that mean MDA8 ozone during July-August has decreased by 23%, from
679 48 ppb in 2004 to 37 ppb in 2013. Despite a positive absolute bias of up to 12 ppb in

boundary layer ozone and 16 ppb in surface MDA8 ozone, our model shows a 10 ppb decrease of surface MDA8 ozone from 2004 to 2013, very close to the observed 11 ppb decrease from the EPA data. The bias of ozone in our model is not entirely attributed to uncertainties in NO_x emissions, as the overestimate suggested by earlier work would lead to an underestimate of NO_y (Travis et al., 2016). Care should be exercised in applying the modeling results for surface ozone regulation purposes, given the high ozone bias shown in our model. We find from model calculations that modeled MDA8 O_3 will continue to decrease by another 9 ppb assuming anthropogenic NO_x emissions are reduced by 40 % from 2013 levels with meteorology and other emissions kept the same. In addition, further NO_x emission reduction leads to less frequent high ozone events. This continued strong sensitivity of surface O_3 to NO_x emissions can guide the development of effective emission control strategies for improving future air quality.

Data availability

Observational datasets and modeling results are available upon request to the corresponding author (jmao2@alaska.edu).

Competing interests

The authors declare that they have no conflict of interest.

Acknowledgements

The authors thank Vaishali Naik (NOAA GFDL) for providing emission inventories in the GFDL AM3 model, and Leo Donner (NOAA GFDL) and William Cooke (UCAR/NOAA) for the help with convection scheme of AM3. J.L., J.M. and L.W.H. acknowledge support from the NOAA Climate Program Office grant # NA13OAR431007. J.M., L.W.H. and A.M.F. acknowledge support from NOAA Climate Program Office grant #NA14OAR4310133. J.D.C. and P.O.W. acknowledge support from NASA grants (NNX12AC06G and NNX14AP46G). J.L acknowledge support from the Startup Foundation for Introducing Talent of NUIST grant #2243141701014 and the Priority Academic Program Development of Jiangsu Higher Education Institutions (PAPD).

References

Anderson, D. C., Loughner, C. P., Diskin, G., Weinheimer, A., Canty, T. P., Salawitch, R. J., Worden, H. M., Fried, A., Mikoviny, T., Wisthaler, A., and Dickerson, R. R.: Measured and modeled CO and NOy in DISCOVER-AQ: An evaluation of emissions and chemistry over the eastern US, Atmos. Environ., 96, 78-87, 2014.

Appel, K., Foley, K., Bash, J., Pinder, R., Dennis, R., Allen, D., and Pickering, K.: A multi-resolution assessment of the Community Multiscale Air Quality (CMAQ) model v4. 7 wet deposition estimates for 2002–2006, Geosci. Model. Dev., 4, 2, 357-371, 2011.

Aschmann, S. M., Atkinson, R., and Arey, J.: Products of reaction of OH radicals with α - pinene, J. Geophys. Res., 107, D14, 2002.

Astitha, M., Luo, H., Rao, S. T., Hogrefe, C., Mathur, R., and Kumar, N.: Dynamic evaluation of two decades of WRF-CMAQ ozone simulations over the contiguous United States, Atmos. Environ., 164, Supplement C, 102-116, 2017.

Ayres, B. R., Allen, H. M., Draper, D. C., Brown, S. S., Wild, R. J., Jimenez, J. L., Day, D. A., Campuzano-Jost, P., Hu, W., de Gouw, J., Koss, A., Cohen, R. C., Duffey, K. C., Romer, P., Baumann, K., Edgerton, E., Takahama, S., Thornton, J. A., Lee, B. H., Lopez-Hilfiker, F. D., Mohr, C., Wennberg, P. O., Nguyen, T. B., Teng, A., Goldstein, A. H., Olson, K., and Fry, J. L.: Organic nitrate aerosol formation via NO3 + biogenic volatile organic compounds in the southeastern United States, Atmos. Chem. Phys., 15, 23, 13377-13392, 2015.

Baker, K. R., and Woody, M. C.: Assessing Model Characterization of Single Source Secondary Pollutant Impacts Using 2013 SENEX Field Study Measurements, Environ. Sci. Technol., 51, 7, 3833-3842, 2017.

Bates, K. H., Crounse, J. D., St. Clair, J. M., Bennett, N. B., Nguyen, T. B., Seinfeld, J. H., Stoltz, B. M., and Wennberg, P. O.: Gas Phase Production and Loss of Isoprene Epoxydiols, J. Phys. Chem. A, 118, 7, 1237-1246, 2014.

Bates, K. H., Nguyen, T. B., Teng, A. P., Crounse, J. D., Kjaergaard, H. G., Stoltz, B. M., Seinfeld, J. H., and Wennberg, P. O.: Production and Fate of C4 Dihydroxycarbonyl Compounds from Isoprene Oxidation, J. Phys. Chem. A, 120, 1, 106-117, 2016.

Bean, J. K., and Hildebrandt Ruiz, L.: Gas–particle partitioning and hydrolysis of organic nitrates formed from the oxidation of α-pinene in environmental chamber experiments, Atmos. Chem. Phys., 16, 4, 2175-2184, 2016.

Blanchard, C. L., Hidy, G. M., Shaw, S., Baumann, K., and Edgerton, E. S.: Effects of emission reductions on organic aerosol in the southeastern United States, Atmos. Chem. Phys., 16, 1, 215-238, 2016.

Bloomer, B. J., Vinnikov, K. Y., and Dickerson, R. R.: Changes in seasonal and diurnal cycles of ozone and temperature in the eastern U.S, Atmos. Environ., 44, 21–22, 2543-2551, 2010.

Boyd, C. M., Sanchez, J., Xu, L., Eugene, A. J., Nah, T., Tuet, W. Y., Guzman, M. I., and Ng, N. L.: Secondary organic aerosol formation from the β-pinene+NO3 system: effect of humidity and peroxy radical fate, Atmos. Chem. Phys., 15, 13, 7497-7522, 2015.

Boyd, C. M., Nah, T., Xu, L., Berkemeier, T., and Ng, N. L.: Secondary Organic Aerosol (SOA) from Nitrate Radical Oxidation of Monoterpenes: Effects of Temperature, Dilution, and Humidity on Aerosol Formation, Mixing, and Evaporation, Environ. Sci. Technol., 51, 14, 7831-7841, 2017.

Brown-Steiner, B., Hess, P. G., and Lin, M. Y.: On the capabilities and limitations of GCCM simulations of summertime regional air quality: A diagnostic analysis of ozone and temperature simulations in the US using CESM CAM-Chem, Atmos. Environ., 101, 134-148, 2015.

Browne, E. C., and Cohen, R. C.: Effects of biogenic nitrate chemistry on the NOx lifetime in remote continental regions, Atmos. Chem. Phys., 12, 24, 11917-11932, 2012.

Browne, E. C., Wooldridge, P. J., Min, K. E., and Cohen, R. C.: On the role of monoterpene chemistry in the remote continental boundary layer, Atmos. Chem. Phys., 14, 3, 1225-1238, 2014.

Camalier, L., Cox, W., and Dolwick, P.: The effects of meteorology on ozone in urban areas and their use in assessing ozone trends, Atmos. Environ., 41, 33, 7127-7137, 2007.

Canty, T. P., Hembeck, L., Vinciguerra, T. P., Anderson, D. C., Goldberg, D. L., Carpenter, S. F., Allen, D. J., Loughner, C. P., Salawitch, R. J., and Dickerson, R. R.: Ozone and NOx chemistry in the eastern US: evaluation of CMAQ/CB05 with satellite (OMI) data, Atmos. Chem. Phys., 15, 4, 4427-4461, 2015.

Cooper, O. R., Gao, R.-S., Tarasick, D., Leblanc, T., and Sweeney, C.: Long-term ozone trends at rural ozone monitoring sites across the United States, 1990–2010, J. Geophys. Res., 117, D22307, 2012.

Crounse, J. D., Paulot, F., Kjaergaard, H. G., and Wennberg, P. O.: Peroxy radical isomerization in the oxidation of isoprene, Phys. Chem. Chem. Phys., 13, 30, 13607-13613, 2011.

Darer, A. I., Cole-Filipiak, N. C., O'Connor, A. E., and Elrod, M. J.: Formation and Stability of Atmospherically Relevant Isoprene-Derived Organosulfates and Organonitrates, Environ. Sci. Technol., 45, 5, 1895-1902, 2011.

Donner, L. J., Wyman, B. L., Hemler, R. S., Horowitz, L. W., Ming, Y., Zhao, M., Golaz, J.-C., Ginoux, P., Lin, S.-J., Schwarzkopf, M. D., Austin, J., Alaka, G., Cooke, W. F., Delworth, T. L., Freidenreich, S. M., Gordon, C. T., Griffies, S. M., Held, I. M., Hurlin,

W. J., Klein, S. A., Knutson, T. R., Langenhorst, A. R., Lee, H.-C., Lin, Y., Magi, B. I., Malyshev, S. L., Milly, P. C. D., Naik, V., Nath, M. J., Pincus, R., Ploshay, J. J., Ramaswamy, V., Seman, C. J., Shevliakova, E., Sirutis, J. J., Stern, W. F., Stouffer, R. J., Wilson, R. J., Winton, M., Wittenberg, A. T., and Zeng, F.: The Dynamical Core, Physical Parameterizations, and Basic Simulation Characteristics of the Atmospheric Component AM3 of the GFDL Global Coupled Model CM3, J. Climate, 24, 13, 3484-3519, 2011.

Edwards, P. M., Aikin, K. C., Dube, W. P., Fry, J. L., Gilman, J. B., de Gouw, J. A., Graus, M. G., Hanisco, T. F., Holloway, J., Hubler, G., Kaiser, J., Keutsch, F. N., Lerner, B. M., Neuman, J. A., Parrish, D. D., Peischl, J., Pollack, I. B., Ravishankara, A. R., Roberts, J. M., Ryerson, T. B., Trainer, M., Veres, P. R., Wolfe, G. M., Warneke, C., and Brown, S. S.: Transition from high- to low-NOx control of night-time oxidation in the southeastern US, Nature Geosci, 10, 7, 490-495, 2017.

Fang, Y., Fiore, A. M., Horowitz, L., Levy, H., Hu, Y., and Russell, A.: Sensitivity of the NOy budget over the United States to anthropogenic and lightning NOx in summer, J. Geophys. Res., 115, D18, 2010.

Fehsenfeld, F. C., Ancellet, G., Bates, T. S., Goldstein, A. H., Hardesty, R. M., Honrath, R., Law, K. S., Lewis, A. C., Leaitch, R., McKeen, S., Meagher, J., Parrish, D. D., Pszenny, A. A. P., Russell, P. B., Schlager, H., Seinfeld, J., Talbot, R., and Zbinden, R.: International Consortium for Atmospheric Research on Transport and Transformation (ICARTT): North America to Europe—Overview of the 2004 summer field study, J. Geophys. Res., 111, D23S01, 2006.

Fiore, A. M., Horowitz, L. W., Purves, D. W., Levy, H., Evans, M. J., Wang, Y., Li, Q., and Yantosca, R. M.: Evaluating the contribution of changes in isoprene emissions to surface ozone trends over the eastern United States, J. Geophys. Res., 110, D12303, 2005.

Fiore, A. M., Dentener, F. J., Wild, O., Cuvelier, C., Schultz, M. G., Hess, P., Textor, C., Schulz, M., Doherty, R. M., and Horowitz, L. W.: Multimodel estimates of intercontinental source‐receptor relationships for ozone pollution, J. Geophys. Res., 114, D4, 83-84, 2009.

Fischer, E., Jacob, D. J., Yantosca, R. M., Sulprizio, M. P., Millet, D., Mao, J., Paulot, F., Singh, H., Roiger, A., and Ries, L.: Atmospheric peroxyacetyl nitrate (PAN): a global budget and source attribution, Atmos. Chem. Phys., 14, 5, 2679-2698, 2014.

Fisher, J. A., Jacob, D. J., Travis, K. R., Kim, P. S., Marais, E. A., Miller, C. C., Yu, K., Zhu, L., Yantosca, R. M., and Sulprizio, M. P.: Organic nitrate chemistry and its implications for nitrogen budgets in an isoprene- and monoterpene-rich atmosphere: constraints from aircraft (SEAC4RS) and ground-based (SOAS) observations in the Southeast US, Atmos. Chem. Phys., 16, 1, 1-38, 2016.

817 Fry, J. L., Kiendler-Scharr, A., Rollins, A. W., Wooldridge, P. J., Brown, S. S., Fuchs,
818 H., Dubé, W., Mensah, A., dal Maso, M., Tillmann, R., Dorn, H. P., Brauers, T., and
819 Cohen, R. C.: Organic nitrate and secondary organic aerosol yield from NO3 oxidation of
820 β-pinene evaluated using a gas-phase kinetics/aerosol partitioning model, Atmos. Chem.
821 Phys., 9, 4, 1431-1449, 2009.

822 Fry, J. L., Draper, D. C., Barsanti, K. C., Smith, J. N., Ortega, J., Winkler, P. M., Lawler,
823 M. J., Brown, S. S., Edwards, P. M., Cohen, R. C., and Lee, L.: Secondary Organic
824 Aerosol Formation and Organic Nitrate Yield from NO3 Oxidation of Biogenic
825 Hydrocarbons, Environ. Sci. Technol., 48, 20, 11944-11953, 2014.

826 Granier, C., Bessagnet, B., Bond, T., D'Angiola, A., Denier van der Gon, H., Frost, G. J.,
827 Heil, A., Kaiser, J. W., Kinne, S., Klimont, Z., Kloster, S., Lamarque, J.-F., Liousse, C.,
828 Masui, T., Meleux, F., Mieville, A., Ohara, T., Raut, J.-C., Riahi, K., Schultz, M. G.,
829 Smith, S. J., Thompson, A., van Aardenne, J., van der Werf, G. R., and van Vuuren, D.
830 P.: Evolution of anthropogenic and biomass burning emissions of air pollutants at global
831 and regional scales during the 1980–2010 period, Clim. Change, 109, 1, 163-190, 2011.

832 Grimm, J. W., and Lynch, J. A.: Improved daily precipitation nitrate and ammonium
833 concentration models for the Chesapeake Bay Watershed, Environ. Pollut., 135, 3, 445-
834 455, 2005.

835 Hardacre, C., Wild, O., and Emberson, L.: An evaluation of ozone dry deposition in
836 global scale chemistry climate models, Atmos. Chem. Phys., 15, 11, 6419-6436, 2015.

837 Henderson, B. H., Pinder, R. W., Crooks, J., Cohen, R. C., Hutzell, W. T., Sarwar, G.,
838 Goliff, W. S., Stockwell, W. R., Fahr, A., Mathur, R., Carlton, A. G., and Vizuete, W.:
839 Evaluation of simulated photochemical partitioning of oxidized nitrogen in the upper
840 troposphere, Atmos. Chem. Phys., 11, 1, 275-291, 2011.

841 Hidy, G. M., Blanchard, C. L., Baumann, K., Edgerton, E., Tanenbaum, S., Shaw, S.,
842 Knipping, E., Tombach, I., Jansen, J., and Walters, J.: Chemical climatology of the
843 southeastern United States, 1999-2013, Atmos. Chem. Phys., 14, 21, 11893-11914, 2014.

844 Hidy, G. M., and Blanchard, C. L.: Precursor reductions and ground-level ozone in the
845 Continental United States, J. Air Waste Manag. Assoc., 65, 10, 1261-1282, 2015.

846 Horowitz, L. W., Liang, J., Gardner, G. M., and Jacob, D. J.: Export of reactive nitrogen
847 from North America during summertime: Sensitivity to hydrocarbon chemistry, J.
848 Geophys. Res., 103, D11, 13451-13476, 1998.

849 Horowitz, L. W., Fiore, A. M., Milly, G. P., Cohen, R. C., Perring, A., Wooldridge, P. J.,
850 Hess, P. G., Emmons, L. K., and Lamarque, J.-F.: Observational constraints on the
851 chemistry of isoprene nitrates over the eastern United States, J. Geophys. Res., 112,
852 D12S08, 2007.

853 Hu, K. S., Darer, A. I., and Elrod, M. J.: Thermodynamics and kinetics of the hydrolysis
854 of atmospherically relevant organonitrates and organosulfates, Atmos. Chem. Phys., 11,
855 16, 8307-8320, 2011.

856 Hudman, R., Jacob, D. J., Cooper, O., Evans, M., Heald, C., Park, R., Fehsenfeld, F.,
857 Flocke, F., Holloway, J., and Hübler, G.: Ozone production in transpacific Asian
858 pollution plumes and implications for ozone air quality in California, J. Geophys. Res.,
859 109, D23, 2004.

860 Hudman, R. C., Jacob, D. J., Turquety, S., Leibensperger, E. M., Murray, L. T., Wu, S.,
861 Gilliland, A. B., Avery, M., Bertram, T. H., Brune, W., Cohen, R. C., Dibb, J. E., Flocke,
862 F. M., Fried, A., Holloway, J., Neuman, J. A., Orville, R., Perring, A., Ren, X., Sachse,
863 G. W., Singh, H. B., Swanson, A., and Wooldridge, P. J.: Surface and lightning sources
864 of nitrogen oxides over the United States: Magnitudes, chemical evolution, and outflow,
865 J. Geophys. Res., 112, D12S05, 2007.

866 Hudman, R. C., Murray, L. T., Jacob, D. J., Turquety, S., Wu, S., Millet, D. B., Avery,
867 M., Goldstein, A. H., and Holloway, J.: North American influence on tropospheric ozone
868 and the effects of recent emission reductions: Constraints from ICARTT observations, J.
869 Geophys. Res., 114, D7, 2009.

870 Hudman, R. C., Moore, N. E., Mebust, A. K., Martin, R. V., Russell, A. R., Valin, L. C.,
871 and Cohen, R. C.: Steps towards a mechanistic model of global soil nitric oxide
872 emissions: implementation and space based-constraints, Atmos. Chem. Phys., 12, 16,
873 7779-7795, 2012.

874 Ito, A., Sillman, S., and Penner, J. E.: Global chemical transport model study of ozone
875 response to changes in chemical kinetics and biogenic volatile organic compounds
876 emissions due to increasing temperatures: Sensitivities to isoprene nitrate chemistry and
877 grid resolution, J. Geophys. Res., 114, D09301, 2009.

878 Jacob, D. J., and Winner, D. A.: Effect of climate change on air quality, Atmos. Environ.,
879 43, 1, 51-63, 2009.

880 Jacobs, M. I., Burke, W. J., and Elrod, M. J.: Kinetics of the reactions of isoprene-derived
881 hydroxynitrates: gas phase epoxide formation and solution phase hydrolysis, Atmos.
882 Chem. Phys., 14, 17, 8933-8946, 2014.

883 Jenkin, M. E., Young, J. C., and Rickard, A. R.: The MCM v3.3.1 degradation scheme
884 for isoprene, Atmos. Chem. Phys., 15, 20, 11433-11459, 2015.

885 Kavassalis, S., and Murphy, J. G.: Understanding ozone-meteorology correlations: a role
886 for dry deposition, Geophys. Res. Lett.10.1002/2016GL071791, 2017.

887 Krotkov, N. A., McLinden, C. A., Li, C., Lamsal, L. N., Celarier, E. A., Marchenko, S.
888 V., Swartz, W. H., Bucsela, E. J., Joiner, J., Duncan, B. N., Boersma, K. F., Veefkind, J.
889 P., Levelt, P. F., Fioletov, V. E., Dickerson, R. R., He, H., Lu, Z., and Streets, D. G.:

Aura OMI observations of regional SO2 and NO2 pollution changes from 2005 to 2015, Atmos. Chem. Phys., 16, 7, 4605-4629, 2016.

Lam, Y., Fu, J., Wu, S., and Mickley, L.: Impacts of future climate change and effects of biogenic emissions on surface ozone and particulate matter concentrations in the United States, Atmos. Chem. Phys., 11, 10, 4789-4806, 2011.

Lamarque, J.-F., Kyle, G. P., Meinshausen, M., Riahi, K., Smith, S. J., van Vuuren, D. P., Conley, A. J., and Vitt, F.: Global and regional evolution of short-lived radiatively-active gases and aerosols in the Representative Concentration Pathways, Clim. Change, 109, 1, 191-212, 2011.

Lamsal, L. N., Duncan, B. N., Yoshida, Y., Krotkov, N. A., Pickering, K. E., Streets, D. G., and Lu, Z.: U.S. NO2 trends (2005–2013): EPA Air Quality System (AQS) data versus improved observations from the Ozone Monitoring Instrument (OMI), Atmos. Environ., 110, 130-143, 2015.

Lee, B. H., Mohr, C., Lopez-Hilfiker, F. D., Lutz, A., Hallquist, M., Lee, L., Romer, P., Cohen, R. C., Iyer, S., Kurtén, T., Hu, W., Day, D. A., Campuzano-Jost, P., Jimenez, J. L., Xu, L., Ng, N. L., Guo, H., Weber, R. J., Wild, R. J., Brown, S. S., Koss, A., de Gouw, J., Olson, K., Goldstein, A. H., Seco, R., Kim, S., McAvey, K., Shepson, P. B., Starn, T., Baumann, K., Edgerton, E. S., Liu, J., Shilling, J. E., Miller, D. O., Brune, W., Schobesberger, S., D'Ambro, E. L., and Thornton, J. A.: Highly functionalized organic nitrates in the southeast United States: Contribution to secondary organic aerosol and reactive nitrogen budgets, Proc. Natl. Acad. Sci. U.S.A., 113, 6, 1516-1521, 2016.

Lee, L., Teng, A. P., Wennberg, P. O., Crounse, J. D., and Cohen, R. C.: On Rates and Mechanisms of OH and O3 Reactions with Isoprene-Derived Hydroxy Nitrates, J. Phys. Chem. A, 118, 9, 1622-1637, 2014.

Li, J., Mao, J., Min, K.-E., Washenfelder, R. A., Brown, S. S., Kaiser, J., Keutsch, F. N., Volkamer, R., Wolfe, G. M., Hanisco, T. F., Pollack, I. B., Ryerson, T. B., Graus, M., Gilman, J. B., Lerner, B. M., Warneke, C., de Gouw, J. A., Middlebrook, A. M., Liao, J., Welti, A., Henderson, B. H., McNeill, V. F., Hall, S. R., Ullmann, K., Donner, L. J., Paulot, F., and Horowitz, L. W.: Observational constraints on glyoxal production from isoprene oxidation and its contribution to organic aerosol over the Southeast United States, J. Geophys. Res., 121, 16, 2016JD025331, 2016.

Li, Q., Jacob, D. J., Munger, J. W., Yantosca, R. M., and Parrish, D. D.: Export of NOy from the North American boundary layer: Reconciling aircraft observations and global model budgets, J. Geophys. Res., 109, D2, 2004.

Liang, J., Horowitz, L. W., Jacob, D. J., Wang, Y., Fiore, A. M., Logan, J. A., Gardner, G. M., and Munger, J. W.: Seasonal budgets of reactive nitrogen species and ozone over the United States, and export fluxes to the global atmosphere, J. Geophys. Res., 103, D11, 13435-13450, 1998.

928 Lin, M., Horowitz, L. W., Payton, R., Fiore, A. M., and Tonnesen, G.: US surface ozone
929 trends and extremes from 1980 to 2014: quantifying the roles of rising Asian emissions,
930 domestic controls, wildfires, and climate, Atmos. Chem. Phys., 17, 4, 2943-2970, 2017.

931 Liu, X., Zhang, Y., Huey, L. G., Yokelson, R. J., Wang, Y., Jimenez, J. L., Campuzano-
932 Jost, P., Beyersdorf, A. J., Blake, D. R., Choi, Y., St. Clair, J. M., Crounse, J. D., Day, D.
933 A., Diskin, G. S., Fried, A., Hall, S. R., Hanisco, T. F., King, L. E., Meinardi, S.,
934 Mikoviny, T., Palm, B. B., Peischl, J., Perring, A. E., Pollack, I. B., Ryerson, T. B.,
935 Sachse, G., Schwarz, J. P., Simpson, I. J., Tanner, D. J., Thornhill, K. L., Ullmann, K.,
936 Weber, R. J., Wennberg, P. O., Wisthaler, A., Wolfe, G. M., and Ziemba, L. D.:
937 Agricultural fires in the southeastern U.S. during SEAC4RS: Emissions of trace gases
938 and particles and evolution of ozone, reactive nitrogen, and organic aerosol, J. Geophys.
939 Res., 121, 12, 7383-7414, 2016.

940 Lockwood, A. L., Shepson, P. B., Fiddler, M. N., and Alaghmand, M.: Isoprene nitrates:
941 preparation, separation, identification, yields, and atmospheric chemistry, Atmos. Chem.
942 Phys., 10, 13, 6169-6178, 2010.

943 Lu, Z., Streets, D. G., De Foy, B., Lamsal, L. N., Duncan, B. N., and Xing, J.: Emissions
944 of nitrogen oxides from US urban areas: estimation from Ozone Monitoring Instrument
945 retrievals for 2005-2014, Atmos. Chem. Phys., 15, 10, 14961-15003, 2015.

946 Mao, J., Horowitz, L. W., Naik, V., Fan, S., Liu, J., and Fiore, A. M.: Sensitivity of
947 tropospheric oxidants to biomass burning emissions: implications for radiative forcing,
948 Geophys. Res. Lett., 40, 6, 1241-1246, 2013a.

949 Mao, J., Paulot, F., Jacob, D. J., Cohen, R. C., Crounse, J. D., Wennberg, P. O., Keller, C.
950 A., Hudman, R. C., Barkley, M. P., and Horowitz, L. W.: Ozone and organic nitrates over
951 the eastern United States: Sensitivity to isoprene chemistry, J. Geophys. Res., 118, 19,
952 11,256-211,268, 2013b.

953 Metcalfe, S. E., Whyatt, J. D., Nicholson, J. P. G., Derwent, R. G., and Heywood, E.:
954 Issues in model validation: assessing the performance of a regional-scale acid deposition
955 model using measured and modelled data, Atmos. Environ., 39, 4, 587-598, 2005.

956 Millet, D. B., Jacob, D. J., Boersma, K. F., Fu, T. M., Kurosu, T. P., Chance, K., Heald,
957 C. L., and Guenther, A.: Spatial Distribution of Isoprene Emissions from North America
958 Derived from Dormaldehyde Column Measurements by the OMI Satellite Sensor, J.
959 Geophys. Res., 113, D2, 194-204, 2008.

960 Miyazaki, K., Eskes, H., Sudo, K., Boersma, K. F., Bowman, K., and Kanaya, Y.:
961 Decadal changes in global surface NOx emissions from multi-constituent satellite data
962 assimilation, Atmos. Chem. Phys., 17, 2, 807-837, 2017.

963 Moxim, W., Levy, H., and Kasibhatla, P.: Simulated global tropospheric PAN: Its
964 transport and impact on NO x, J. Geophys. Res., 101, D7, 12621-12638, 1996.

Müller, J. F., Peeters, J., and Stavrakou, T.: Fast photolysis of carbonyl nitrates from isoprene, Atmos. Chem. Phys., 14, 5, 2497-2508, 2014.

Nah, T., Sanchez, J., Boyd, C. M., and Ng, N. L.: Photochemical Aging of α-pinene and β-pinene Secondary Organic Aerosol formed from Nitrate Radical Oxidation, Environ. Sci. Technol., 50, 1, 222-231, 2016.

Naik, V., Horowitz, L. W., Fiore, A. M., Ginoux, P., Mao, J., Aghedo, A. M., and Levy, H.: Impact of preindustrial to present-day changes in short-lived pollutant emissions on atmospheric composition and climate forcing, J. Geophys. Res., 118, 14, 8086-8110, 2013.

Neuman, J., Parrish, D., Trainer, M., Ryerson, T., Holloway, J., Nowak, J., Swanson, A., Flocke, F., Roberts, J., and Brown, S.: Reactive nitrogen transport and photochemistry in urban plumes over the North Atlantic Ocean, J. Geophys. Res., 111, D23, 2006.

Ng, N. L., Kwan, A. J., Surratt, J. D., Chan, A. W. H., Chhabra, P. S., Sorooshian, A., Pye, H. O. T., Crounse, J. D., Wennberg, P. O., Flagan, R. C., and Seinfeld, J. H.: Secondary organic aerosol (SOA) formation from reaction of isoprene with nitrate radicals (NO3), Atmos. Chem. Phys., 8, 14, 4117-4140, 2008.

Ng, N. L., Brown, S. S., Archibald, A. T., Atlas, E., Cohen, R. C., Crowley, J. N., Day, D. A., Donahue, N. M., Fry, J. L., Fuchs, H., Griffin, R. J., Guzman, M. I., Herrmann, H., Hodzic, A., Iinuma, Y., Jimenez, J. L., Kiendler-Scharr, A., Lee, B. H., Luecken, D. J., Mao, J., McLaren, R., Mutzel, A., Osthoff, H. D., Ouyang, B., Picquet-Varrault, B., Platt, U., Pye, H. O. T., Rudich, Y., Schwantes, R. H., Shiraiwa, M., Stutz, J., Thornton, J. A., Tilgner, A., Williams, B. J., and Zaveri, R. A.: Nitrate radicals and biogenic volatile organic compounds: oxidation, mechanisms, and organic aerosol, Atmos. Chem. Phys., 17, 3, 2103-2162, 2017.

Nguyen, T. B., Crounse, J. D., Teng, A. P., St. Clair, J. M., Paulot, F., Wolfe, G. M., and Wennberg, P. O.: Rapid deposition of oxidized biogenic compounds to a temperate forest, Proc. Natl. Acad. Sci. U.S.A., 112, 5, E392-E401, 2015.

Nozière, B., Barnes, I., and Becker, K. H.: Product study and mechanisms of the reactions of α - pinene and of pinonaldehyde with OH radicals, J. Geophys. Res., 104, D19, 23645-23656, 1999.

Ott, L. E., Pickering, K. E., Stenchikov, G. L., Allen, D. J., DeCaria, A. J., Ridley, B., Lin, R.-F., Lang, S., and Tao, W.-K.: Production of lightning NOx and its vertical distribution calculated from three-dimensional cloud-scale chemical transport model simulations, J. Geophys. Res., 115, D4, 2010.

Parrish, D., Ryerson, T., Holloway, J., Neuman, J., Roberts, J., Williams, J., Stroud, C., Frost, G., Trainer, M., and Hübler, G.: Fraction and composition of NOy transported in air masses lofted from the North American continental boundary layer, J. Geophys. Res., 109, D9, 2004.

1003 Paulot, F., Crounse, J. D., Kjaergaard, H. G., Kroll, J. H., Seinfeld, J. H., and Wennberg,
1004 P. O.: Isoprene photooxidation: new insights into the production of acids and organic
1005 nitrates, Atmos. Chem. Phys., 9, 4, 1479-1501, 2009.

1006 Paulot, F., Henze, D. K., and Wennberg, P. O.: Impact of the isoprene photochemical
1007 cascade on tropical ozone, Atmos. Chem. Phys., 12, 3, 1307-1325, 2012.

1008 Paulot, F., Jacob, D. J., Pinder, R. W., Bash, J. O., Travis, K., and Henze, D. K.:
1009 Ammonia emissions in the United States, European Union, and China derived by high-
1010 resolution inversion of ammonium wet deposition data: Interpretation with a new
1011 agricultural emissions inventory (MASAGE_NH3), J. Geophys. Res., 119, 7, 4343-4364,
1012 2014.

1013 Paulot, F., Ginoux, P., Cooke, W. F., Donner, L. J., Fan, S., Lin, M. Y., Mao, J., Naik, V.,
1014 and Horowitz, L. W.: Sensitivity of nitrate aerosols to ammonia emissions and to nitrate
1015 chemistry: implications for present and future nitrate optical depth, Atmos. Chem. Phys.,
1016 16, 3, 1459-1477, 2016.

1017 Peeters, J., Müller, J.-F., Stavrakou, T., and Nguyen, V. S.: Hydroxyl Radical Recycling
1018 in Isoprene Oxidation Driven by Hydrogen Bonding and Hydrogen Tunneling: The
1019 Upgraded LIM1 Mechanism, J. Phys. Chem. A, 118, 38, 8625-8643, 2014.

1020 Perring, A. E., Bertram, T. H., Wooldridge, P. J., Fried, A., Heikes, B. G., Dibb, J.,
1021 Crounse, J. D., Wennberg, P. O., Blake, N. J., Blake, D. R., Brune, W. H., Singh, H. B.,
1022 and Cohen, R. C.: Airborne observations of total RONO2: new constraints on the yield
1023 and lifetime of isoprene nitrates, Atmos. Chem. Phys., 9, 4, 1451-1463, 2009.

1024 Perring, A. E., Pusede, S. E., and Cohen, R. C.: An Observational Perspective on the
1025 Atmospheric Impacts of Alkyl and Multifunctional Nitrates on Ozone and Secondary
1026 Organic Aerosol, Chem. Rev., 113, 8, 5848-5870, 2013.

1027 Philip, S., Martin, R. V., and Keller, C. A.: Sensitivity of chemistry-transport model
1028 simulations to the duration of chemical and transport operators: a case study with GEOS-
1029 Chem v10-01, Geosci. Model Dev., 9, 5, 1683-1695, 2016.

1030 Pickering, K. E., Wang, Y., Tao, W. K., Price, C., and Müller, J. F.: Vertical distributions
1031 of lightning NOx for use in regional and global chemical transport models, J. Geophys.
1032 Res., 103, D23, 31203–31216, 1998.

1033 Pierce, R. B., Schaack, T., Al-Saadi, J. A., Fairlie, T. D., Kittaka, C., Lingenfelser, G.,
1034 Natarajan, M., Olson, J., Soja, A., Zapotocny, T., Lenzen, A., Stobie, J., Johnson, D.,
1035 Avery, M. A., Sachse, G. W., Thompson, A., Cohen, R., Dibb, J. E., Crawford, J., Rault,
1036 D., Martin, R., Szykman, J., and Fishman, J.: Chemical data assimilation estimates of
1037 continental U.S. ozone and nitrogen budgets during the Intercontinental Chemical
1038 Transport Experiment–North America, J. Geophys. Res., 112, D12, 2007.

1039 Pollack, I. B., Ryerson, T. B., Trainer, M., Neuman, J., Roberts, J. M., and Parrish, D. D.:
1040 Trends in ozone, its precursors, and related secondary oxidation products in Los Angeles,

California: A synthesis of measurements from 1960 to 2010, J. Geophys. Res., 118, 11, 5893-5911, 2013.

Praske, E., Crounse, J. D., Bates, K. H., Kurtén, T., Kjaergaard, H. G., and Wennberg, P. O.: Atmospheric Fate of Methyl Vinyl Ketone: Peroxy Radical Reactions with NO and HO2, J. Phys. Chem. A, 119, 19, 4562-4572, 2015.

Pye, H. O. T., Luecken, D. J., Xu, L., Boyd, C. M., Ng, N. L., Baker, K. R., Ayres, B. R., Bash, J. O., Baumann, K., Carter, W. P. L., Edgerton, E., Fry, J. L., Hutzell, W. T., Schwede, D. B., and Shepson, P. B.: Modeling the Current and Future Roles of Particulate Organic Nitrates in the Southeastern United States, Environ. Sci. Technol., 49, 24, 14195-14203, 2015.

Rieder, H. E., Fiore, A. M., Horowitz, L. W., and Naik, V.: Projecting policy - relevant metrics for high summertime ozone pollution events over the eastern United States due to climate and emission changes during the 21st century, J. Geophys. Res., 120, 2, 784-800, 2015.

Rindelaub, J. D., McAvey, K. M., and Shepson, P. B.: The photochemical production of organic nitrates from α-pinene and loss via acid-dependent particle phase hydrolysis, Atmos. Environ., 100, 193-201, 2015.

Rindelaub, J. D., Borca, C. H., Hostetler, M. A., Slade, J. H., Lipton, M. A., Slipchenko, L. V., and Shepson, P. B.: The acid-catalyzed hydrolysis of an α-pinene-derived organic nitrate: kinetics, products, reaction mechanisms, and atmospheric impact, Atmos. Chem. Phys., 16, 23, 15425-15432, 2016.

Rollins, A. W., Kiendler-Scharr, A., Fry, J. L., Brauers, T., Brown, S. S., Dorn, H. P., Dubé, W. P., Fuchs, H., Mensah, A., Mentel, T. F., Rohrer, F., Tillmann, R., Wegener, R., Wooldridge, P. J., and Cohen, R. C.: Isoprene oxidation by nitrate radical: alkyl nitrate and secondary organic aerosol yields, Atmos. Chem. Phys., 9, 18, 6685-6703, 2009.

Rollins, A. W., Smith, J. D., Wilson, K. R., and Cohen, R. C.: Real Time In Situ Detection of Organic Nitrates in Atmospheric Aerosols, Environ. Sci. Technol., 44, 14, 5540-5545, 2010.

Romer, P. S., Duffey, K. C., Wooldridge, P. J., Allen, H. M., Ayres, B. R., Brown, S. S., Brune, W. H., Crounse, J. D., de Gouw, J., Draper, D. C., Feiner, P. A., Fry, J. L., Goldstein, A. H., Koss, A., Misztal, P. K., Nguyen, T. B., Olson, K., Teng, A. P., Wennberg, P. O., Wild, R. J., Zhang, L., and Cohen, R. C.: The lifetime of nitrogen oxides in an isoprene-dominated forest, Atmos. Chem. Phys., 16, 12, 7623-7637, 2016.

Russell, A. R., Valin, L. C., and Cohen, R. C.: Trends in OMI NO2 observations over the United States: effects of emission control technology and the economic recession, Atmos. Chem. Phys., 12, 24, 12197-12209, 2012.

Sanderson, M., Dentener, F., Fiore, A., Cuvelier, C., Keating, T., Zuber, A., Atherton, C., Bergmann, D., Diehl, T., and Doherty, R.: A multi‐model study of the hemispheric transport and deposition of oxidised nitrogen, Geophys. Res. Lett., 35, 17, 2008.

Sato, K.: Detection of nitrooxypolyols in secondary organic aerosol formed from the photooxidation of conjugated dienes under high-NOx conditions, Atmos. Environ., 42, 28, 6851-6861, 2008.

Schwantes, R. H., Teng, A. P., Nguyen, T. B., Coggon, M. M., Crounse, J. D., St. Clair, J. M., Zhang, X., Schilling, K. A., Seinfeld, J. H., and Wennberg, P. O.: Isoprene NO3 Oxidation Products from the RO2 + HO2 Pathway, J. Phys. Chem. A, 119, 40, 10158-10171, 2015.

Sillman, S.: Ozone production efficiency and loss of NO x in power plant plumes: Photochemical model and interpretation of measurements in Tennessee, J. Geophys. Res., 105, D7, 9189-9202, 2000.

Simon, H., Reff, A., Wells, B., Xing, J., and Frank, N.: Ozone Trends Across the United States over a Period of Decreasing NOx and VOC Emissions, Environ. Sci. Technol., 49, 1, 186-195, 2015.

Singh, H. B., Brune, W. H., Crawford, J. H., Jacob, D. J., and Russell, P. B.: Overview of the summer 2004 Intercontinental Chemical Transport Experiment–North America (INTEX-A), J. Geophys. Res., 111, D24S01, 2006.

Singh, H. B., Salas, L., Herlth, D., Kolyer, R., Czech, E., Avery, M., Crawford, J. H., Pierce, R. B., Sachse, G. W., Blake, D. R., Cohen, R. C., Bertram, T. H., Perring, A., Wooldridge, P. J., Dibb, J., Huey, G., Hudman, R. C., Turquety, S., Emmons, L. K., Flocke, F., Tang, Y., Carmichael, G. R., and Horowitz, L. W.: Reactive nitrogen distribution and partitioning in the North American troposphere and lowermost stratosphere, J. Geophys. Res., 112, D12, 2007.

Spittler, M., Barnes, I., Bejan, I., Brockmann, K. J., Benter, T., and Wirtz, K.: Reactions of NO3 radicals with limonene and α-pinene: Product and SOA formation, Atmos. Environ., 40, 116-127, 2006.

St. Clair, J. M., Rivera-Rios, J. C., Crounse, J. D., Knap, H. C., Bates, K. H., Teng, A. P., Jørgensen, S., Kjaergaard, H. G., Keutsch, F. N., and Wennberg, P. O.: Kinetics and Products of the Reaction of the First-Generation Isoprene Hydroxy Hydroperoxide (ISOPOOH) with OH, J. Phys. Chem. A, 120, 9, 1441-1451, 2016.

Steiner, A. L., Davis, A. J., Sillman, S., Owen, R. C., Michalak, A. M., and Fiore, A. M.: Observed suppression of ozone formation at extremely high temperatures due to chemical and biophysical feedbacks, Proc. Natl. Acad. Sci. U.S.A., 107, 46, 19685-19690, 2010.

Stoeckenius, T. E., Hogrefe, C., Zagunis, J., Sturtz, T. M., Wells, B., and Sakulyanontvittaya, T.: A comparison between 2010 and 2006 air quality and

meteorological conditions, and emissions and boundary conditions used in simulations of the AQMEII-2 North American domain, Atmos. Environ., 115, 389-403, 2015.

Stohl, A., Trainer, M., Ryerson, T. B., Holloway, J. S., and Parrish, D. D.: Export of NOy from the North American boundary layer during 1996 and 1997 North Atlantic Regional Experiments, J. Geophys. Res., 107, D11, ACH 11-11-ACH 11-13, 2002.

Strode, S. A., Rodriguez, J. M., Logan, J. A., Cooper, O. R., Witte, J. C., Lamsal, L. N., Damon, M., Van Aartsen, B., Steenrod, S. D., and Strahan, S. E.: Trends and variability in surface ozone over the United States, J. Geophys. Res., 120, 17, 9020-9042, 2015.

Szmigielski, R., Vermeylen, R., Dommen, J., Metzger, A., Maenhaut, W., Baltensperger, U., and Claeys, M.: The acid effect in the formation of 2-methyltetrols from the photooxidation of isoprene in the presence of NOx, Atmos. Res., 98, 2–4, 183-189, 2010.

Tawfik, A. B., and Steiner, A. L.: A proposed physical mechanism for ozone-meteorology correlations using land–atmosphere coupling regimes, Atmos. Environ., 72, 50-59, 2013.

Teng, A., Crounse, J., Lee, L., St Clair, J., Cohen, R., and Wennberg, P.: Hydroxy nitrate production in the OH-initiated oxidation of alkenes, Atmos. Chem. Phys., 15, 8, 4297-4316, 2015.

Tong, D. Q., Lamsal, L., Pan, L., Ding, C., Kim, H., Lee, P., Chai, T., Pickering, K. E., and Stajner, I.: Long-term NOx trends over large cities in the United States during the great recession: Comparison of satellite retrievals, ground observations, and emission inventories, Atmos. Environ., 107, 70-84, 2015.

Toon, O. B., Maring, H., Dibb, J., Ferrare, R., Jacob, D. J., Jensen, E. J., Luo, Z. J., Mace, G. G., Pan, L. L., Pfister, L., Rosenlof, K. H., Redemann, J., Reid, J. S., Singh, H. B., Thompson, A. M., Yokelson, R., Minnis, P., Chen, G., Jucks, K. W., and Pszenny, A.: Planning, implementation and scientific goals of the Studies of Emissions and Atmospheric Composition, Clouds and Climate Coupling by Regional Surveys (SEAC4RS) field mission, J. Geophys. Res., 121, 4967-5009, 2016.

Tost, H., Jöckel, P., Kerkweg, A., Pozzer, A., Sander, R., and Lelieveld, J.: Global cloud and precipitation chemistry and wet deposition: tropospheric model simulations with ECHAM5/MESSy1, Atmos. Chem. Phys., 7, 10, 2733-2757, 2007.

Trainer, M., Parrish, D. D., Goldan, P. D., Roberts, J., and Fehsenfeld, F. C.: Review of observation-based analysis of the regional factors influencing ozone concentrations, Atmos. Environ., 34, 12–14, 2045-2061, 2000.

Travis, K. R., Jacob, D. J., Fisher, J. A., Kim, P. S., Marais, E. A., Zhu, L., Yu, K., Miller, C. C., Yantosca, R. M., Sulprizio, M. P., Thompson, A. M., Wennberg, P. O., Crounse, J. D., St. Clair, J. M., Cohen, R. C., Laughner, J. L., Dibb, J. E., Hall, S. R., Ullmann, K., Wolfe, G. M., Pollack, I. B., Peischl, J., Neuman, J. A., and Zhou, X.: Why

do models overestimate surface ozone in the Southeast United States?, Atmos. Chem. Phys., 16, 21, 13561-13577, 2016.

Val Martin, M., Heald, C. L., and Arnold, S. R.: Coupling dry deposition to vegetation phenology in the Community Earth System Model: Implications for the simulation of surface O 3, Geophys. Res. Lett., 41, 8, 2988–2996, 2014.

Warneke, C., Trainer, M., de Gouw, J. A., Parrish, D. D., Fahey, D. W., Ravishankara, A. R., Middlebrook, A. M., Brock, C. A., Roberts, J. M., Brown, S. S., Neuman, J. A., Lerner, B. M., Lack, D., Law, D., Hübler, G., Pollack, I., Sjostedt, S., Ryerson, T. B., Gilman, J. B., Liao, J., Holloway, J., Peischl, J., Nowak, J. B., Aikin, K. C., Min, K. E., Washenfelder, R. A., Graus, M. G., Richardson, M., Markovic, M. Z., Wagner, N. L., Welti, A., Veres, P. R., Edwards, P., Schwarz, J. P., Gordon, T., Dube, W. P., McKeen, S. A., Brioude, J., Ahmadov, R., Bougiatioti, A., Lin, J. J., Nenes, A., Wolfe, G. M., Hanisco, T. F., Lee, B. H., Lopez-Hilfiker, F. D., Thornton, J. A., Keutsch, F. N., Kaiser, J., Mao, J., and Hatch, C. D.: Instrumentation and measurement strategy for the NOAA SENEX aircraft campaign as part of the Southeast Atmosphere Study 2013, Atmos. Meas. Tech., 9, 7, 3063-3093, 2016.

Wolfe, G., Hanisco, T., Arkinson, H., Bui, T., Crounse, J., Dean‐Day, J., Goldstein, A., Guenther, A., Hall, S., and Huey, G.: Quantifying sources and sinks of reactive gases in the lower atmosphere using airborne flux observations, Geophys. Res. Lett., 42, 19, 8231-8240, 2015.

Wu, S., Mickley, L. J., Jacob, D. J., Rind, D., and Streets, D. G.: Effects of 2000–2050 changes in climate and emissions on global tropospheric ozone and the policy-relevant background surface ozone in the United States, J. Geophys. Res., 113, D18312, 2008.

Xing, J., Mathur, R., Pleim, J., Hogrefe, C., Gan, C. M., Wong, D. C., Wei, C., Gilliam, R., and Pouliot, G.: Observations and modeling of air quality trends over 1990–2010 across the Northern Hemisphere: China, the United States and Europe, Atmos. Chem. Phys., 15, 5, 2723-2747, 2015.

Xiong, F., McAvey, K. M., Pratt, K. A., Groff, C. J., Hostetler, M. A., Lipton, M. A., Starn, T. K., Seeley, J. V., Bertman, S. B., Teng, A. P., Crounse, J. D., Nguyen, T. B., Wennberg, P. O., Misztal, P. K., Goldstein, A. H., Guenther, A. B., Koss, A. R., Olson, K. F., de Gouw, J. A., Baumann, K., Edgerton, E. S., Feiner, P. A., Zhang, L., Miller, D. O., Brune, W. H., and Shepson, P. B.: Observation of isoprene hydroxynitrates in the southeastern United States and implications for the fate of NOx, Atmos. Chem. Phys., 15, 19, 11257-11272, 2015.

Xiong, F., Borca, C. H., Slipchenko, L. V., and Shepson, P. B.: Photochemical degradation of isoprene-derived 4,1-nitrooxy enal, Atmos. Chem. Phys., 16, 9, 5595-5610, 2016.

Xu, L., Suresh, S., Guo, H., Weber, R. J., and Ng, N. L.: Aerosol characterization over the southeastern United States using high-resolution aerosol mass spectrometry: spatial

and seasonal variation of aerosol composition and sources with a focus on organic nitrates, Atmos. Chem. Phys., 15, 13, 7307-7336, 2015.

Yahya, K., Wang, K., Campbell, P., Glotfelty, T., He, J., and Zhang, Y.: Decadal evaluation of regional climate, air quality, and their interactions over the continental US and their interactions using WRF/Chem version 3.6.1, Geosci. Model Dev., 9, 2, 671-695, 2016.

Yienger, J. J., and Levy, H. I.: Empirical model of soil-biogenic NOx emissions, J. Geophys. Res., 1001, D6, 11447-11464, 1995.

Yu, K., Jacob, D. J., Fisher, J. A., Kim, P. S., Marais, E. A., Miller, C. C., Travis, K. R., Zhu, L., Yantosca, R. M., Sulprizio, M. P., Cohen, R. C., Dibb, J. E., Fried, A., Mikoviny, T., Ryerson, T. B., Wennberg, P. O., and Wisthaler, A.: Sensitivity to grid resolution in the ability of a chemical transport model to simulate observed oxidant chemistry under high-isoprene conditions, Atmos. Chem. Phys., 16, 7, 4369-4378, 2016.

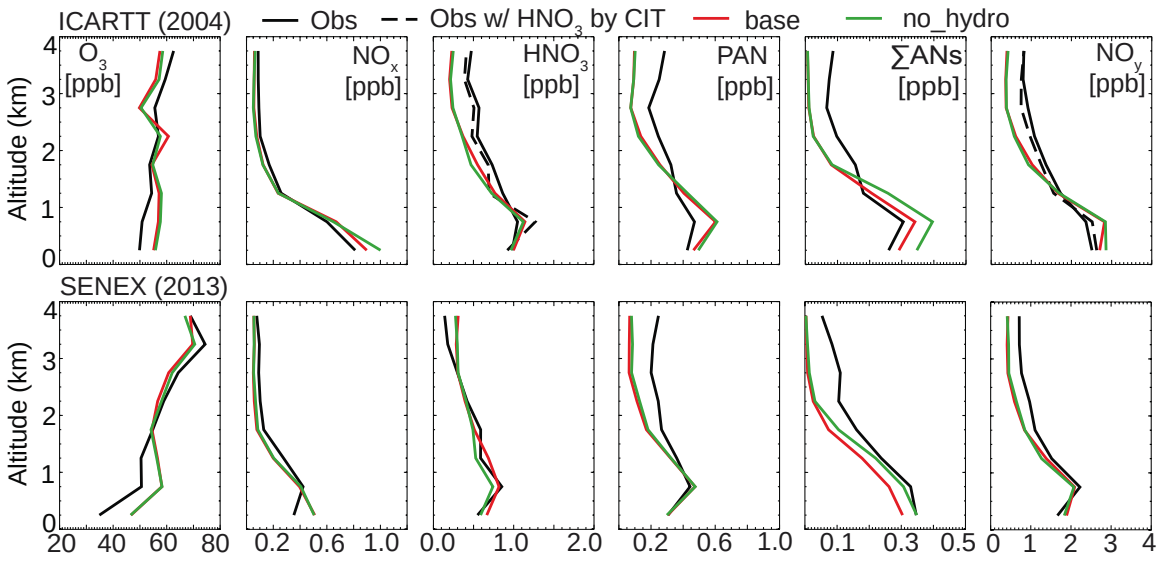

1204

1205 **Figure 1**. Mean vertical profiles of ozone and reactive oxidized nitrogen from observations
1206 during ICARTT (top row) and SENEX (bottom row) over SEUS (25 - 40° N, 100 - 75° W)
1207 during daytime, and model estimates from AM3 with hydrolysis of ISOPNB (red) and
1208 AM3 without hydrolysis of alkyl nitrates (green). The solid and dashed black lines in the
1209 HNO_3 of ICARTT represent measurements collected using mist chamber/IC by University
1210 of New Hampshire (UNH) and Chemical Ionization Mass Spectrometer by California
1211 Institute of Technology (CIT), respectively. NO_y from ICARTT is calculated as the sum of
1212 NO_x, HNO_3 (w/ UNH in the solid line and w/ CIT in the dashed line), PAN and total alkyl
1213 nitrates (∑ANs). ∑ANs in the bottom row are from SEAC^{4}RS.

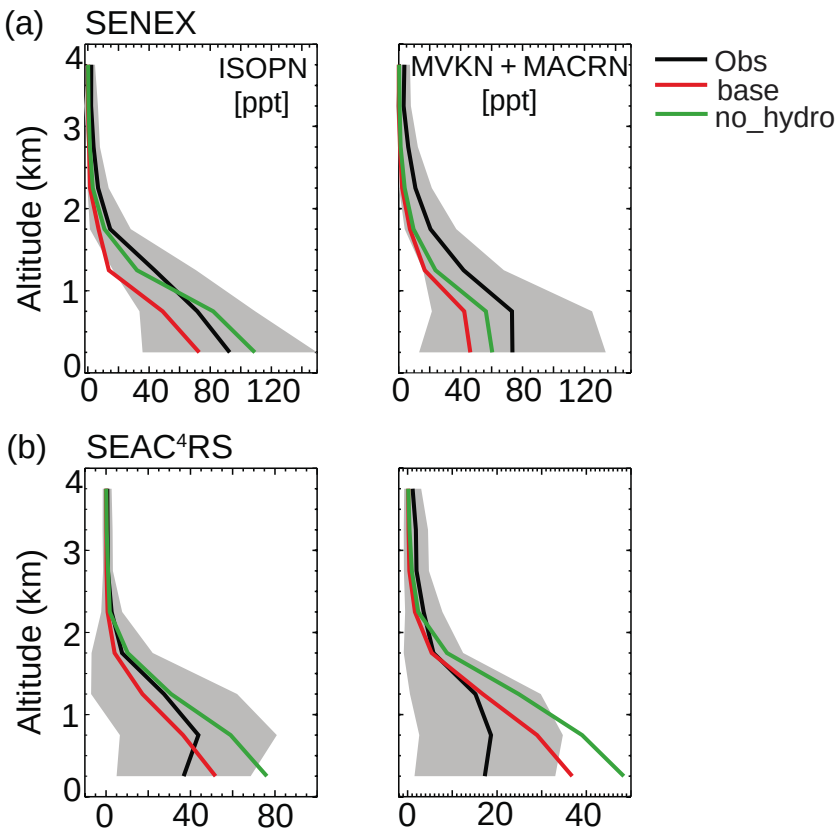

Figure 2. Mean vertical profiles of ISOPN and MVNK+MACRN during (a) SENEX and (b) SEAC^{4}RS over SEUS (25 - 40° N, 100 - 75° W). Black lines are the mean of observations. Red and green lines are the mean of modeled results with hydrolysis of ISOPNB and without hydrolysis of alkyl nitrates respectively. Grey shades are the one standard deviation (±σ) of averaged profiles of the measured tracers.

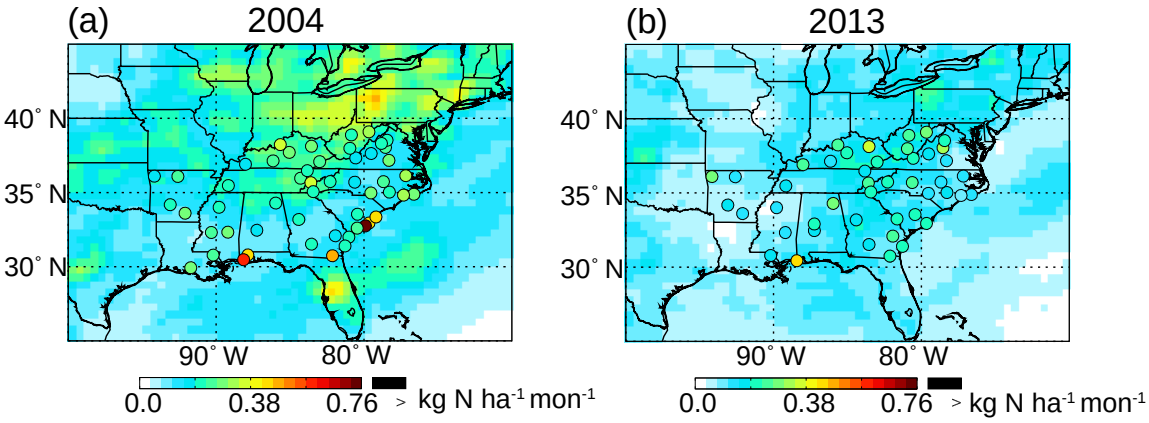

Figure 3. Nitrate wet deposition flux (kg N ha^{-1} mon^{-1}) from NADP (circles) and AM3 (background) during July - August of 2004 and 2013.

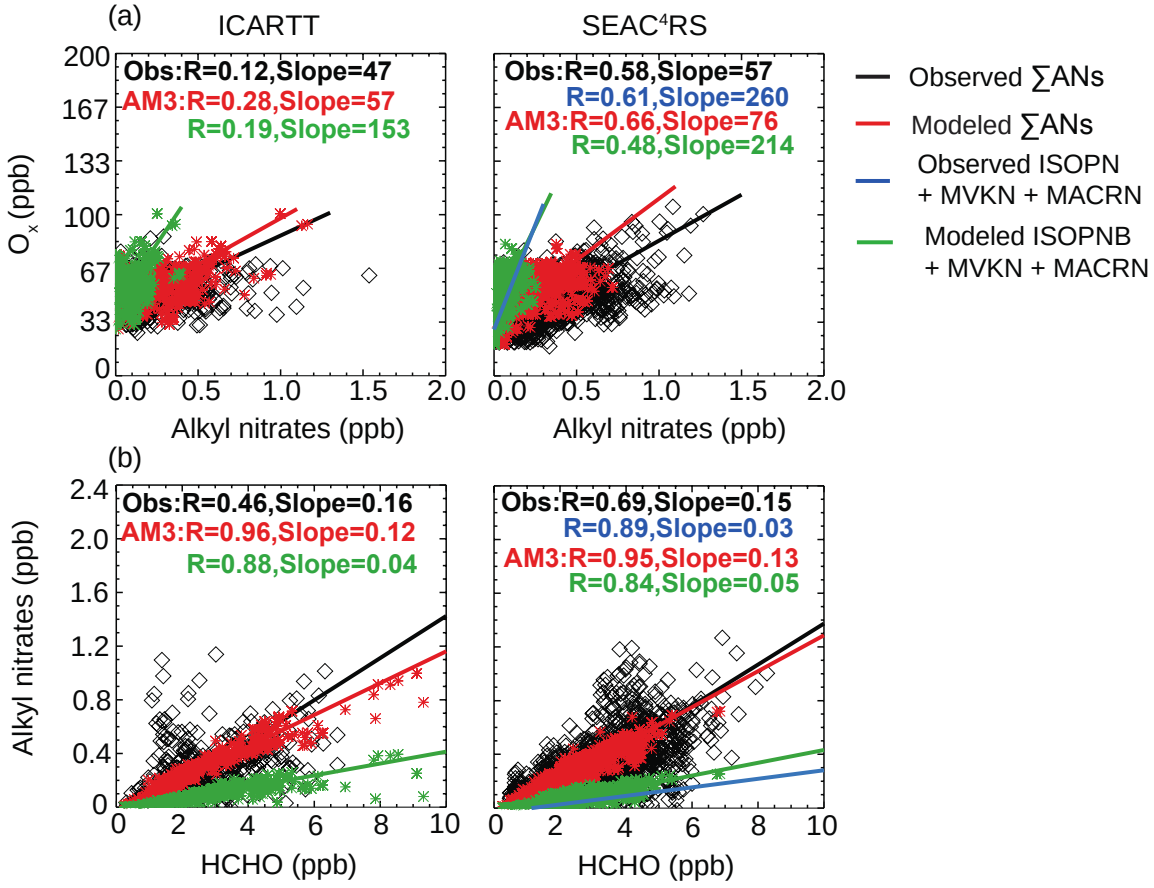

1223

1224 **Figure 4.** O_x versus ∑ANs correlation (top; (a)) and ∑ANs versus formaldehyde
1225 correlation (bottom; (b)) within the boundary layer (< 1.5 km) during ICARTT (left) and
1226 SEAC⁴RS (right). Observations are in black diamonds; model estimates from AM3 with
1227 ISOPNB hydrolysis are in red symbols. Green symbols represent the correlation using
1228 modeled ISOPN + MVKN + MACRN. Blue symbols represent the correlation using
1229 observed ISOPN + MVKN + MACRN from SEAC⁴RS. Solid lines are the reduced major
1230 axis regression lines.

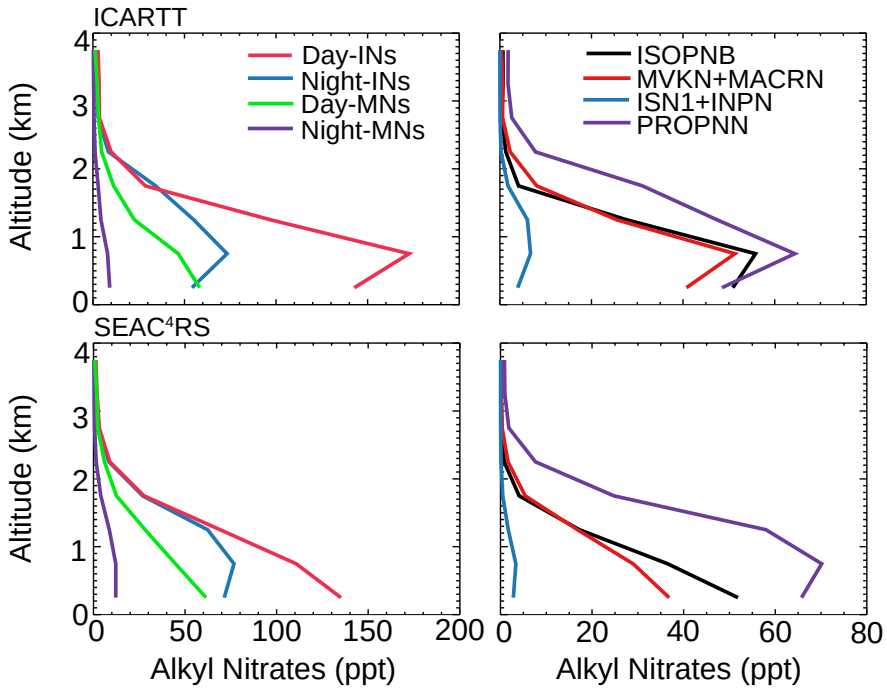

1231

1232 **Figure 5.** Mean vertical profiles of modeled alkyl nitrates from isoprene and monoterpene
1233 oxidation (left) and major isoprene nitrate species (right) during ICARTT (top row) and
1234 SEAC^{4}RS (bottom row) from AM3 with hydrolysis of ISOPNB.

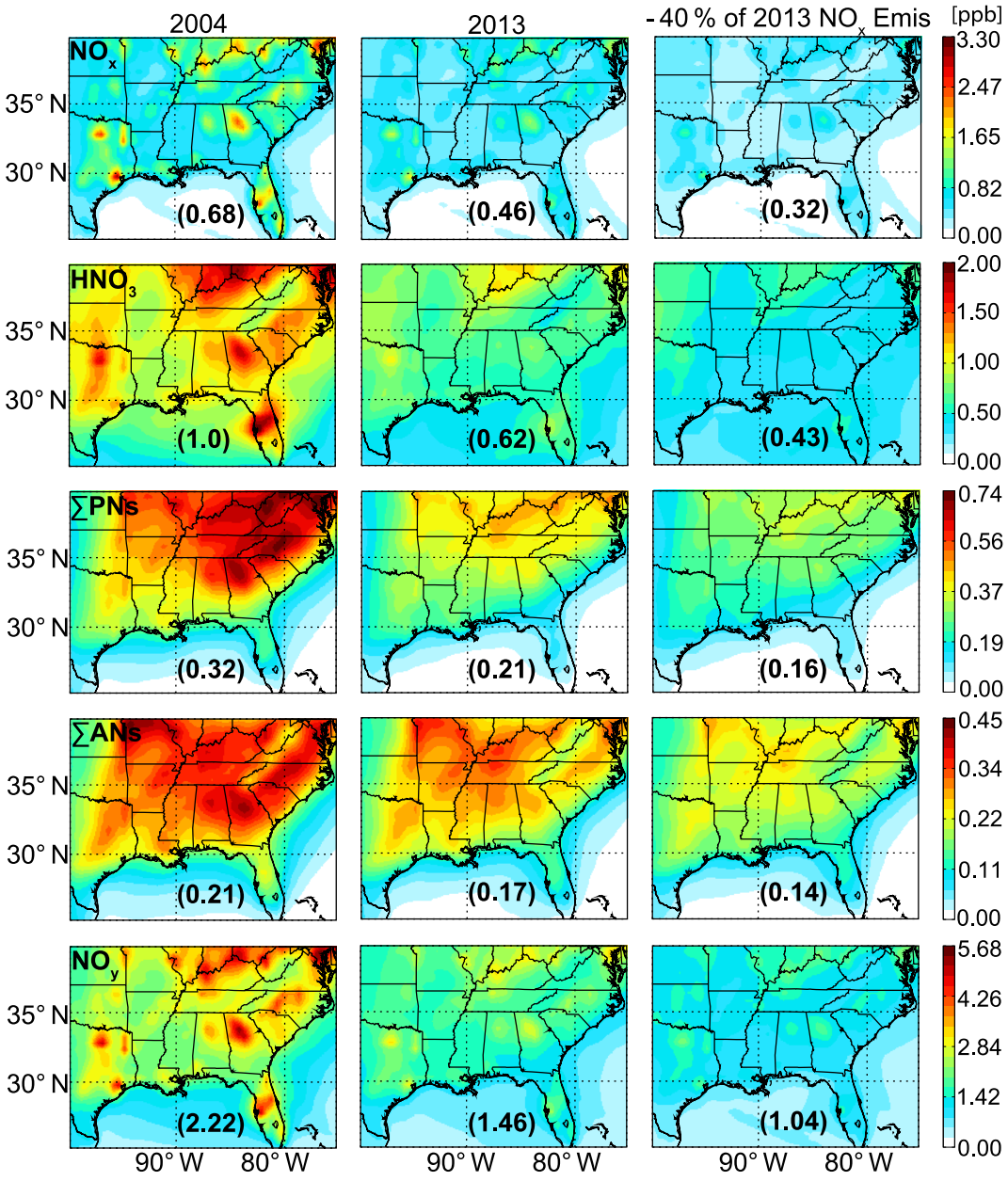

Figure 6. Modeled mean NO_x, HNO_3, total peroxy nitrates (∑PNs), total alkyl nitrates (∑ANs) and NO_y averaged over the boundary layer (< 1.5 km) of the Southeast U.S. during July - August of 2004 (left), 2013 (middle), and a scenario assuming 40 % reduction of 2013 anthropogenic NO_x emissions (right). Numbers in parentheses indicate mean concentrations over the plotted region. Note different color scales represent the concentration of each species.

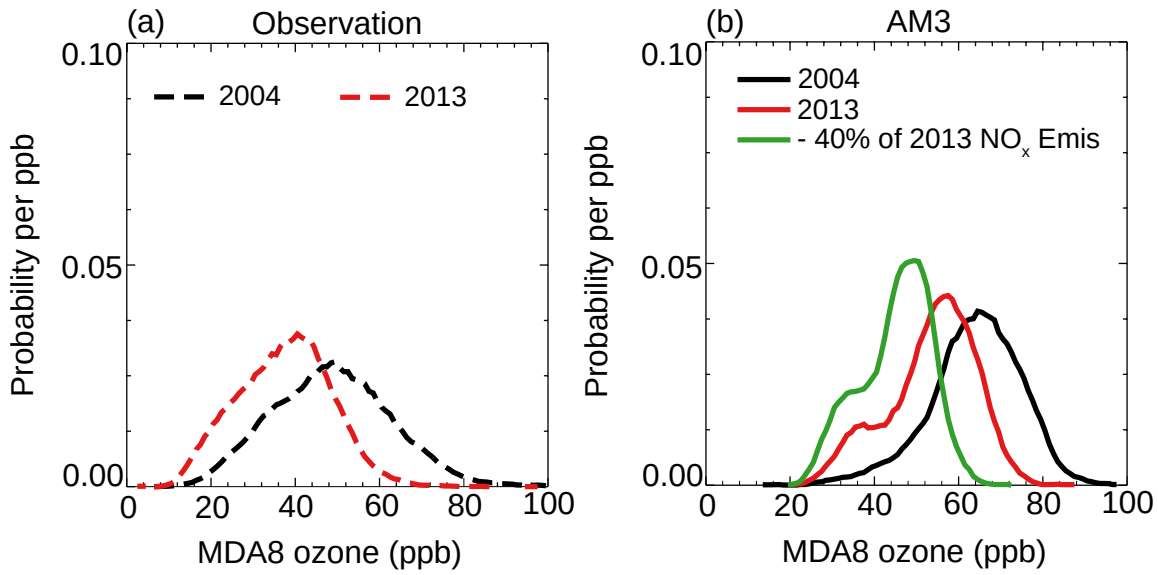

Figure 7. Observed (a) and simulated (b) probability density function of MDA8 ozone at AQS monitoring sites in Figure S3 during summer of 2004, 2013, and a scenario with 40 % reduction in the anthropogenic NO_x emissions of 2013.

Table 1. Monthly averaged NO_x emissions in July-August of 2004 and 2013 over North America (25-50° N, 130-70° W) and over the Southeast US (25-40° N, 100-75° W) in brackets in AM3.

Source Type	2004 (Tg N)	2013 (Tg N)
Anthropogenic	0.42 (0.19)	0.25 (0.11)
Biomass Burning	8.4×10^{-3} (2.8×10^{-3})	8.4×10^{-3} (2.8×10^{-3})
Soils	2.9×10^{-2} (9.5×10^{-3})	2.9×10^{-2} (9.5×10^{-3})
Aircraft	8.8×10^{-3} (2.9×10^{-3})	8.0×10^{-3} (2.8×10^{-3})
Lightning	0.02 (0.01)	0.02 (0.01)
Total	0.49 (0.22)	0.32 (0.14)

1251 **Table 2**. Case descriptions

Case name	Heterogeneous Loss of organic nitrates	NO_x emissions	Meteorology
base	ISOPNB with a γ of 0.005 and followed by a hydrolysis rate of 9.26×10^{-5} s^{-1}	2004 and 2013	2004 and 2013
no_hydro	—	2004 and 2013	2004 and 2013
hydro_full	ISOPNB and DHDN with a γ of 0.005 and followed by a hydrolysis rate of 9.26×10^{-5} s^{-1}; TERPN1 with a γ of 0.01 and followed by a hydrolysis rate of 9.26×10^{-5} s^{-1}	2004 and 2013	2004 and 2013
hypo	Same with the base case	40 % reduction of NO_x emissions of 2013	2013

1252

Table 3. Monthly NO_y budget in the boundary layer (< 1.5 km) of the Southeast United States for July-August of 2004, 2013 and a scenario with 40 % reduction of anthropogenic NO_x emissions of 2013[a].

	2004					2013					- 40 % of 2013 Anthropogenic NO_x Emis				
Species	Emission	Chem (P-L)	Dry Dep	Wet Dep	Net Export	Emission	Chem (P-L)	Dry Dep	Wet Dep	Net Export	Emission	Chem (P-L)	Dry Dep	Wet Dep	Net Export
NO_x	208.7	-172.4	21.8	−	14.5	132.6	-105	14.2	−	13.4	88.3	-69.6	9.2	–	9.5
∑PNs[b]		15.2	5.7	−	9.5		10.3	3.9	−	6.4		7.7	3.0	–	4.7
∑ANs		24.3	14.3	6.2	3.8		19.4	11.4	4.7	3.3		15.4	9.1	3.9	2.4
day[c]		13.8	8.7	3.6	1.5		12.0	7.5	3.0	1.6		10.2	6.3	2.6	1.3
night[d]		10.5	5.6	2.6	2.4		7.4	4.0	1.7	1.7		5.3	2.8	1.3	1.1
HNO_3		131.7	77.8	57.6	-3.7		74.2	45.6	35.1	-6.5		45.8	29.2	25.6	-9.0
NO_y					24.1					16.6					7.6

[a]We define the boundary of Southeast US is 25-40° N, 100-75° W. All budget terms are in Gg N.

[b]∑PNs includes PAN, peroxymethacryloyl nitrate (MPAN), and a C5 hydroxy peroxyacyl nitrate (C5PAN1) produced by oxidation of ISN1.

[c]Alkyl nitrates produced from oxidation of isoprene and monoterpenes by OH.

[d]Alkyl nitrates produced from oxidation of isoprene and monoterpenes by NO_3.